




## RESEARCH ARTICLE

# Recommendations for intervertebral disc notochordal cell investigation: From isolation to characterization

Rebecca J. Williams<sup>1,2</sup> | Lisanne T. Laagland<sup>3</sup>  | Frances C. Bach<sup>3</sup> | Lizzy Ward<sup>4</sup> | Wilson Chan<sup>5</sup> | Vivian Tam<sup>5</sup> | Adel Medzikovic<sup>3</sup> | Shaghayegh Basatvat<sup>1,2</sup> | Lily Paillat<sup>6</sup>  | Nicolas Vedrenne<sup>6</sup> | Joseph W. Snuggs<sup>1,2</sup> | Deepani W. Poramba-Liyanage<sup>3</sup>  | Judith A. Hoyland<sup>4,7</sup> | Danny Chan<sup>5</sup> | Anne Camus<sup>6</sup>  | Stephen M. Richardson<sup>4</sup>  | Marianna A. Tryfonidou<sup>3</sup>  | Christine L. Le Maitre<sup>1,2</sup> 

<sup>1</sup>Department of Oncology and Metabolism, Medical School, The University of Sheffield, Sheffield, UK

<sup>2</sup>Biomolecular Sciences Research Centre, Sheffield Hallam University, Sheffield, UK

<sup>3</sup>Department of Clinical Sciences, Faculty of Veterinary Medicine, Utrecht University, Utrecht, The Netherlands

<sup>4</sup>Division of Cell Matrix Biology and Regenerative Medicine, School of Biological Sciences, Faculty of Biology, Medicine and Health, The University of Manchester, Manchester, UK

<sup>5</sup>School of Biomedical Sciences, The University of Hong Kong, Pokfulam, Hong Kong, China

<sup>6</sup>Regenerative Medicine and Skeleton, RMeS, Nantes Université, Oniris, CHU Nantes, INSERM, UMR 1229, Nantes, France

<sup>7</sup>NIHR Manchester Biomedical Research Centre, Central Manchester Foundation Trust, Manchester Academic Health Science Centre, Manchester, UK

## Correspondence

Christine L. Le Maitre, Department of Oncology and Metabolism, Medical School, The University of Sheffield, Beech Hill Road, Sheffield S10 2RX, UK.

Email: [c.lemaitre@sheffield.ac.uk](mailto:c.lemaitre@sheffield.ac.uk)

## Funding information

European Union's Horizon 2020; iPSpine, Grant/Award Number: 825925; NC-CHOICE, Grant/Award Number: 19251; TTW; Dutch Research Council (NWO); Dutch Arthritis Society, Grant/Award Number: LLP22; RGC European Union – Hong Kong Research and Innovation Cooperation Co-Funding Mechanism, Grant/Award Number: E-HKU703/18; Region Pays de la Loire; RFI BIOREGATE (CAVEODISC); French Society of Rheumatology (Spherodisc)

## Abstract

**Background:** Lineage-tracing experiments have established that the central region of the mature intervertebral disc, the nucleus pulposus (NP), develops from the embryonic structure called “the notochord”. However, changes in the cells derived from the notochord which form the NP (i.e., notochordal cells [NCs]), in terms of their phenotype and functional identity from early developmental stages to skeletal maturation are less understood. These key issues require further investigation to better comprehend the role of NCs in homeostasis and degeneration as well as their potential for regeneration. Progress in utilizing NCs is currently hampered due to poor consistency and lack of consensus methodology for in vitro NC extraction, manipulation, and characterization.

**Methods:** Here, an international group has come together to provide key recommendations and methodologies for NC isolation within key species, numeration, in vitro manipulation and culture, and characterization.

**Results:** Recommended protocols are provided for isolation and culture of NCs. Experimental testing provided recommended methodology for numeration of NCs. The

Lisanne T. Laagland and Frances C. Bach have contributed equally to the study.

This is an open access article under the terms of the [Creative Commons Attribution-NonCommercial](https://creativecommons.org/licenses/by-nc/4.0/) License, which permits use, distribution and reproduction in any medium, provided the original work is properly cited and is not used for commercial purposes.

© 2023 The Authors. *JOR Spine* published by Wiley Periodicals LLC on behalf of Orthopaedic Research Society.

issues of cryopreservation are demonstrated, and a pannel of immunohistochemical markers are provided to inform NC characterization.

**Conclusions:** Together we hope this article provides a road map for in vitro studies of NCs to support advances in research into NC physiology and their potential in regenerative therapies.

#### KEYWORDS

culture systems, development, intervertebral disc, notochordal cells, nucleus pulposus, tissue-specific progenitor cells

## 1 | INTRODUCTION

The notochord is a mesodermal midline structure (also called the axial mesoderm) located along the anterior–posterior axis at the ventral surface of the neural tube and dorsal to the gut, characteristic of chordates.<sup>1,2</sup> It is a transient signaling structure involved in the regionalization and fate of the surrounding embryonic tissues.<sup>3,4</sup> In vertebrates, the notochord plays a key role in signaling and coordinating the development of the vertebral column.<sup>5,6</sup> During development, the notochordal plate folds to develop into the neural tube forming the notochord (ventrally), which is flanked by the paraxial mesoderm and ectoderm (dorsally).<sup>7,8</sup> The paraxial mesoderm goes on to form the somites, which further differentiate into skeletal muscle, connective tissue, dermis, and the sclerotome. The latter eventually gives rise to the ribs, vertebral bodies, cartilaginous end plates (CEPs), and the annulus fibrosus (AF) of the intervertebral disc (IVD).<sup>8–11</sup> Whilst lineage tracing studies in mouse models have demonstrated that the founder cells of the nucleus pulposus (NP), the core of the IVD, originate in the embryonic notochord.<sup>12,13</sup> Once the notochord regresses, notochordal cells (NCs) are restricted to within the NP, and excluded from the forming vertebral bodies.<sup>14</sup>

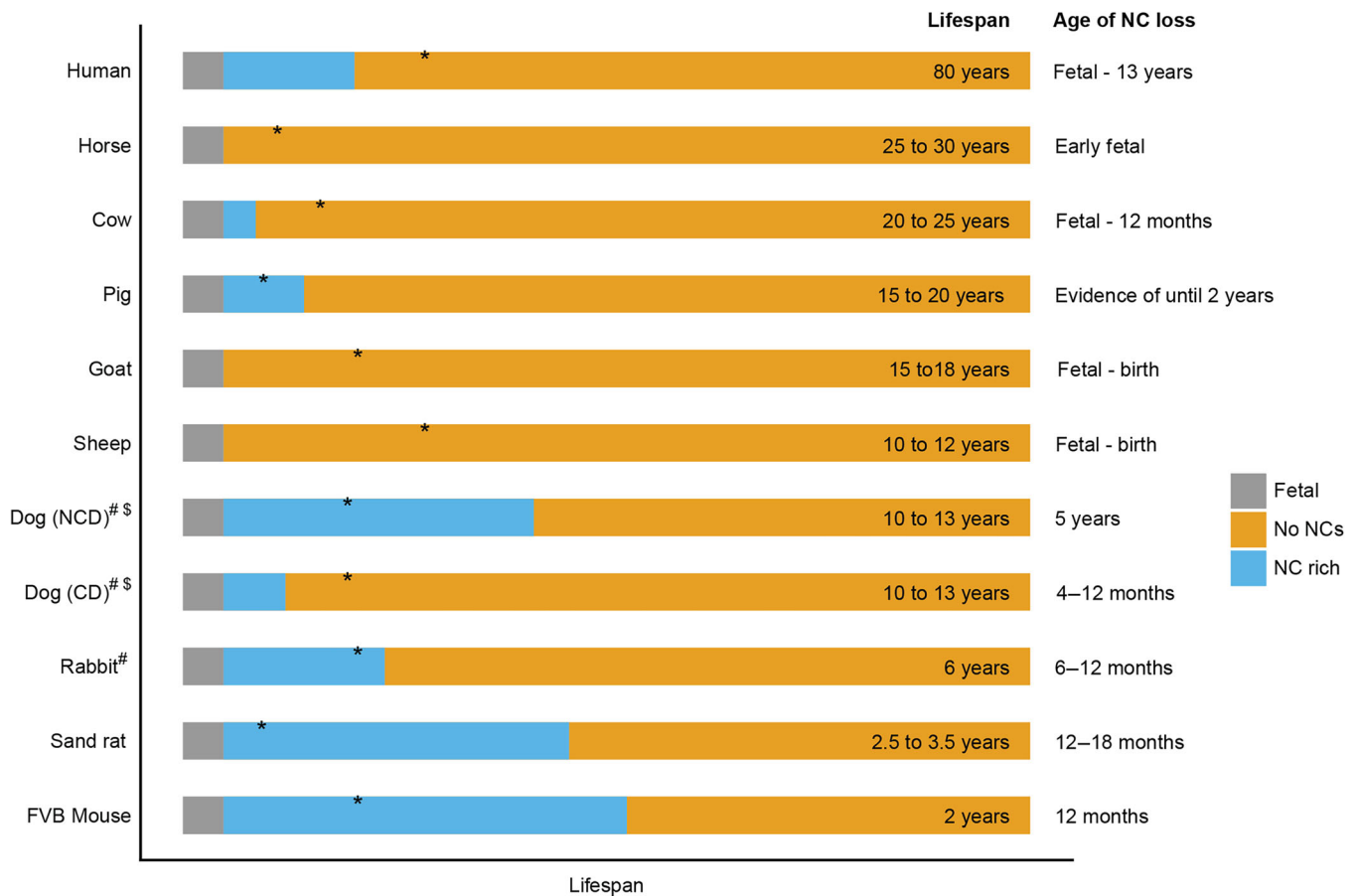
Substantial changes in the cytomorphology and function of NCs are observed throughout morphogenesis, growth, and maturation of the IVD, from its initial state as a notochord primordium to its mature state: the NP of the adult disc. A consensus terminology is currently lacking for defining the notochordal-derived cells within the NP from development to adulthood. Here, we adopt the terminology utilized in Bach et al.,<sup>15</sup> where NCs from the embryonic notochord are defined as embryonic NCs (eNCs), whilst those within the central region of the IVD are termed notochordal cells (NCs).

As well described, at an early stage, the embryonic notochord is composed of large eNCs packed within the perinotochordal sheath consisting of extracellular matrix (ECM) proteins (mainly laminin, proteoglycans, and collagen). eNCs synthesize and secrete collagens and proteoglycans (containing chondroitin 4-sulfate, chondroitin 6-sulfate, and heparan sulfate GAG) which accumulate in the perinotochordal sheath.<sup>16–18</sup> Once these eNCs mature within the NP they exhibit multiple large cytoplasmic vacuoles and eventually differentiate into the NCs. With further NP maturation a transition in cell phenotype takes place from large vacuolated NCs, present in clusters, to smaller and more dispersed nonvacuolated NP cells (NPCs), although the timing of

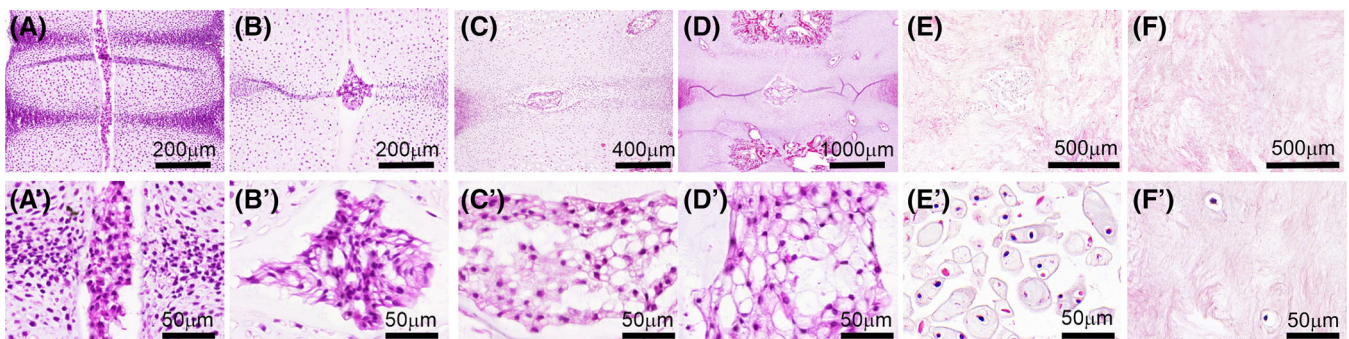
this differs considerably by species (Figure 1).<sup>19–37</sup> The NPCs are phenotypically characterized by their ability to synthesize the appropriate matrisome<sup>38</sup> and can to some extent be identified by specific gene biomarkers.<sup>29,39–41</sup> Although differential gene markers are difficult to identify between the vacuolated NCs and mature nonvacuolated NPCs, the advent of single-cell transcriptomic analysis of these cells provides new perspectives and potential markers.<sup>19,42–45</sup> Thus, further research into developmental studies and NC biology is essential to provide insights into NC-related pathogenesis of IVD degeneration and to understand their potential in IVD regeneration.<sup>8,20,46–49</sup>

The NC population in the NP undergoes species-specific changes (Figure 1). In humans, NCs start to decline before birth (Figures 1 and 2), with complete loss based on their vacuolated morphology by teenage years. Richardson et al.,<sup>19</sup> reported the presence of NC remnants within adolescent human IVDs. Similarly, mature NPs from sheep, goats, and cows contain no NCs, whereas in mice, rabbits, rats, and pigs, the NC population is maintained until much later in life (Figures 1 and 3).<sup>29,50</sup> In dogs, NCs are lost at about 1 year of age in chondrodystrophic breeds (CD; e.g., Beagles and Dachshunds), but remain in the NP until middle/old age in nonchondrodystrophic (NCD) breeds (e.g., Shepherds and Mongrels; Figures 1 and 3).<sup>29,51,52</sup>

The loss of the NC population in certain species (e.g., CD dogs) coincides with the development of IVD degenerative changes and clinical disease,<sup>53</sup> indicating that NCs may play a role in maintaining healthy NP tissue. Several studies<sup>22,54,55</sup> have determined the regenerative potential of NCs and found that they may be a promising target for regenerative and/or symptom-modifying therapies for IVD disease which has been reviewed recently.<sup>15</sup> However, <3% of papers reporting the potential use of cells to promote regeneration of the disc, utilized NCs as the cell choice,<sup>56</sup> whereas a larger emphasis has been on other cell types such as bone marrow-derived mesenchymal stem cells, and mature NP or AF cells. Studies investigating the use of NCs have sourced these from pigs,<sup>55,57–59</sup> rats,<sup>60–62</sup> rabbits,<sup>60</sup> and dogs.<sup>63</sup> The studies mainly utilized 3D in vitro culture, where the phenotype could be maintained at least partially, with a distinct lack of progression into clinical studies. Their limited use in research so far has been due to the difficulties in their utilization in vitro. In particular, maintaining phenotype in monolayer culture in vitro is problematic<sup>55,58,64</sup> and due to their limited capacity to proliferate without loss of phenotype, it is often difficult to harvest sufficient numbers for in vitro manipulation<sup>64–66</sup> and extraction itself often leads to



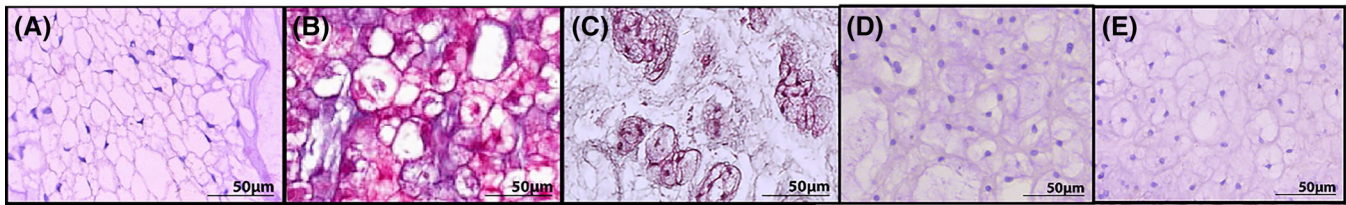
**FIGURE 1** Comparison of the age at which notochordal cells (NCs) are lost from the intervertebral disc. Lifespan refers to approximate lifespan in captivity and can vary depending on environmental factors and other variables. \*Time of skeletal maturity (human 20 years; horse: 2 years; cow: 2–3 years; pig: 12 months; goat: 2–3 years; sheep: 2–3 years; dog [NCD] and dog [CD]: 1–2 years; rabbit: 10 months; sand rat: 2 months; FVB mouse: 4 months). #Depends on breed and genetic background. \$Loss of NCs can depend on breed, genetic background, diet, obesity and injury. In the human, sheep and cow, NC loss begins at fetal stages, with NCs seen at birth. Horse discs in later stages of fetal development are devoid of NCs and none are seen at birth. NC, notochordal cells; CD, chondrodystrophic; NCD, nonchondrodystrophic (References: human<sup>19,20,30–34</sup>; horse<sup>35</sup>; goat<sup>36</sup>; sheep<sup>21,29,37</sup>; cow<sup>22,23</sup>; dog (CD)<sup>24</sup>; dog (NCD)<sup>24,38</sup>; rabbit<sup>25,26,29</sup>; sand rat<sup>27</sup>; FVB mouse<sup>28</sup>).



**FIGURE 2** Notochordal cells within Human Intervertebral discs. Hematoxylin and eosin (H&E)-stained human intervertebral disc (IVD) tissue during development, shown at low and high magnification. Staining demonstrates large vacuolated morphology of cells within the developing nucleus pulposus (NP) region at (A) 7 weeks postconception (wpc), (B) 8.5 wpc, (C) 10 wpc, and (D) 17 wpc. (E) Retention of clusters of large cells within the nucleus pulposus (NP) region in a 10-year-old IVD, whereas (F) shows presence of only single, smaller mature NP cells within the NP region in a 17-year-old IVD.

disruption of normal phenotype.<sup>67</sup> To date, there is a lack of consensus for the extraction, numeration, in vitro culture, and characterization of NCs. Discrepancies observed in results could be explained by

species-specific differences; however, large variations in methodological approaches are likely a major contributor. Thus, this article aims to provide key recommendations and methodologies for NC isolation,



**FIGURE 3** Notochordal cells are maintained in mature discs of mice (A), rats (B), rabbits (C), pigs (D), and some breeds of dogs (E). Images shown are from rodents and pigs <3 months of age, Dog image is from a mixed breed nonchondrodystrophic dog at 1 year of age. Hematoxylin and eosin-stained images, Scale bar = 50  $\mu$ m.

numeration, in vitro manipulation, and characterization to support research into NC physiology and potential in regenerative therapies.

## 2 | RECOMMENDED METHODOLOGY FOR EXTRACTION OF NCS FROM THE NP OF MULTIPLE SPECIES

### 2.1 | Recommendations for dissection and aseptic isolation of IVD/NP tissue

NCS are regularly sourced from several species for in vitro investigations. These include small rodents such as mice and rats where lumbar and caudal (tail) discs are commonly used, however, caudal discs within mice are often preferred due to their higher numbers and ease of accessibility, whilst lumbar and caudal discs are often sourced from rats. However, given the size of rodent IVDs, isolation of pure NP tissue can be problematic and may require downstream fluorescent-activated cell sorting (FACS). Furthermore, generating sufficient cells for downstream analysis normally requires the pooling of discs. Large species such as NCD dogs (IVDs ~20 mm depending on the breed), and pig (IVDs ~30 mm at 3 months) provide large NP tissue sources which are easier to isolate. Within species which lose their NCS during development, that is, humans and CD dogs, fetal (7–25 weeks postconception [wpc] human) or young dog discs are sourced. Dependent on age of the donor, the separation of NP and AF may not be possible in the case of earlier stages of development, like pre segmentation spines, and thus FACS is recommended to ensure pure populations for study.

### 2.2 | Aseptic isolation of the spine/tail

This method outlines the procedure for dissecting the spine or tail (where appropriate) into intact spinal units. However, as some samples, for example, human samples obtained from early pregnancy terminations, are not always received intact, adaptation of this procedure may be required based on the state of the tissue on arrival. To ensure sterility external surfaces such as whole mice, rats, or pig tails/lumbar sections received from the animal house or external sources (i.e., abattoirs) remove first any debris and blood and clean with 70% ethanol (note: only use 70% ethanol if there are tissues external to the IVDs). For isolation of the spinal column of whole

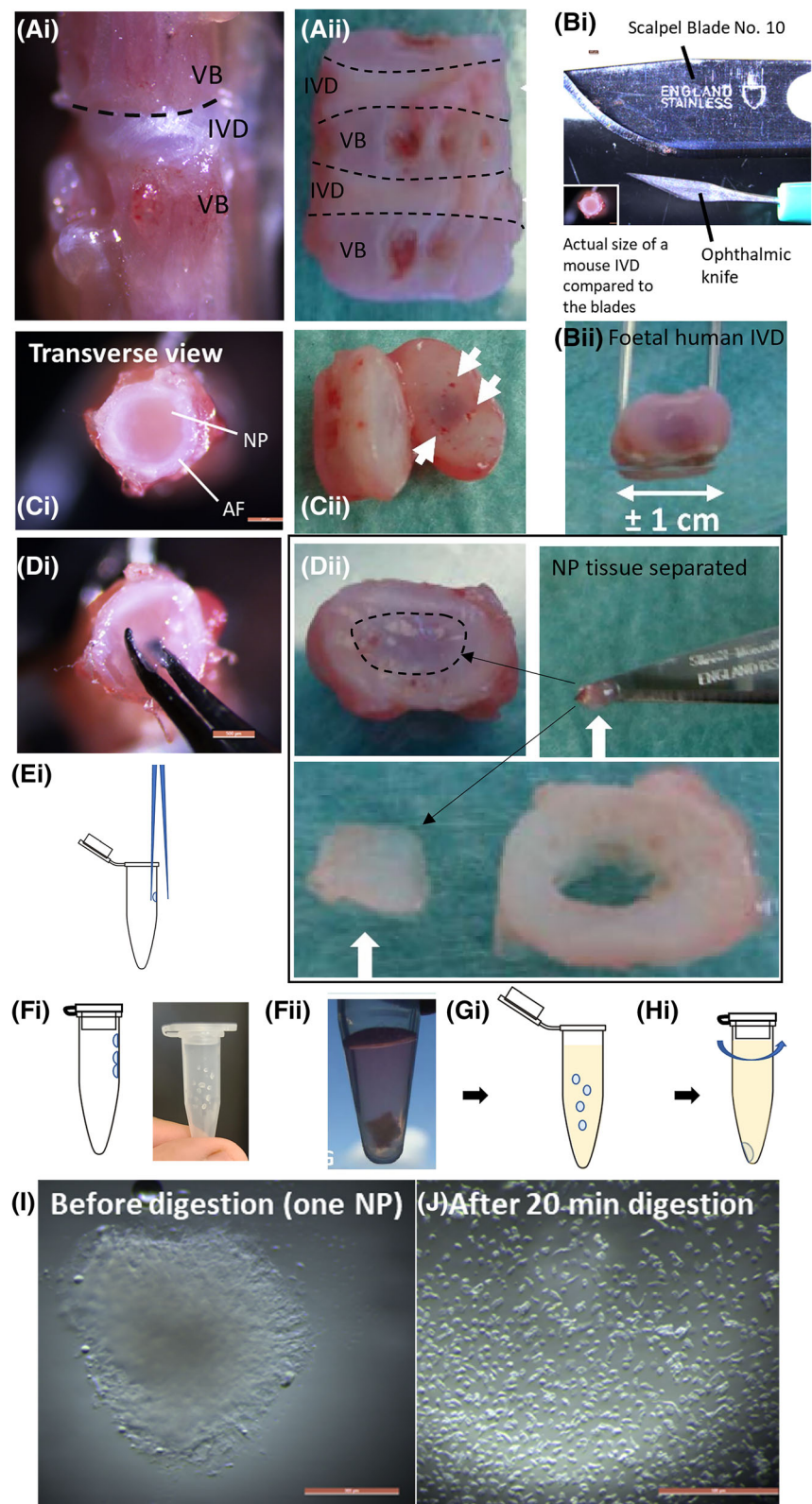
cadavers where available, eviscerate and cutoff the limbs as close to the spine as possible and dissect the spinal column according to the procedure described in detail by Lee et al.,<sup>68</sup> For isolation of caudal discs a longitudinal incision along the dorsal side of the tail is performed to reveal the underlying tissues. Dissect away the skin, muscles, and other tissues exposing the IVDs, whereafter the exterior of the spine/tail is aseptically cleaned according to surgical protocol (two times with Hibiscrub [chlorhexidine gluconate 40 mg/mL]) via spraying with chlorhexidine for two times both followed by 3 min incubation.

### 2.3 | Dissection of the IVD from the spine/tail

For the isolation of IVDs from small specimens, for example, mouse, rat, young dogs, and human fetal samples, IVDs can be seen as bright white stripes between the more translucent vertebral bodies (Figure 4A). It is recommended to use a dissection microscope or binocular glasses to aid with the isolation of the IVD, starting at the most anterior disc. While holding the spine with the fine forceps, use for dissection a microsurgical knife (e.g., nr 11 scalpel knife for larger IVDs) or ophthalmic knives (Beaver® Optimum™ Knives) or an equivalent such as micro blades or a stab knife for small discs such as mouse caudal discs. The stab knife is recommended because discs from mice are very small ~2 mm in diameter and the standard nos. 10/11 scalpel blades are too large and could lead to accidental cutting into the IVD, immediate depressurization of the NP and loss of the tissue (Figure 4B). Cut transversely along the plane of the anterior side of the disc, cutting off the vertebral body adjacent to it (Figure 4C). The disc/vertebral body boundary should be a natural line of least resistance. For younger donors (fetal <18 wpc in humans) where the AF and NP tissues have not undergone segmentation or the vertebrae are not entirely calcified, it may not be possible to isolate the NP tissue from surrounding tissues. In such a case the whole IVD is dissected, and a mixed population of cells isolated which may include NC, AF, and CEP cells which could then be separated using FACS (See section 2.5).

For older donors of NC-rich discs where the NP and AF tissues can easily be distinguished, the AF is seen as a white ring surrounding a translucent jelly-like NP (Figure 4C,D). For mouse discs use a pair of fine-curved forceps to “spoon out” but it is essential you do not pinch the NP tissue from the disc (Note: pinching via standard forceps application will traumatize the tissue and diminish cell viability; Figure 4Di) and place this onto the wall of an empty sterile Eppendorf tube on ice (Figure 4Ei).

**FIGURE 4** Dissection of mouse and stillborn fetal human lumbar spine (21 weeks of gestation). (Ai) Mouse motion segment and (Aii) Human fetal L3, L4, and L5 vertebrae with intervertebral discs (IVDs) L3–L4 and L4–L5. (Bi) Ophthalmic knife and scalpel blade no 10 in comparison to whole mouse IVD demonstrating importance of use of ophthalmic or stab knife for extraction. (Bii) Whole fetal human IVD isolated for scale (1 cm in diameter). (C) The IVD should be excised by cutting at the junction between endplate and annulus fibrosus (AF) shown for mouse (Ci) and human (Cii) IVDs, noted within human fetal IVD end plates with blood vessels (white arrows) can be clearly seen. (D) The nucleus pulposus (NP) region is carefully removed from the IVD in the mouse (Di) this is spooned out with curved forceps, whilst human NP (Dii) can be carefully separated with a nr 11 scalpel blade separating out from the AF and EP tissue. (E) The tissue of the mouse IVD is placed carefully in the edge of an Eppendorf tube and (F) multiple NP tissue samples can be combined together for mouse (Fi) or individual NP tissue may be collected separately for human (Fii) dependent on size. The sample can further be processed by enzymatic digestion (G) prior to centrifugation and resuspension in resuspension media (H). (I) Mouse NP tissue shown pre digestion and (J) after digestion. Scale bar = 500  $\mu$ m.



Whilst for larger discs such as young dog and fetal human ( $> \sim 18$  wpc) discs the NP and AF are separated manually using a curettes size A (World Precision Instruments, 501 773; Figure 4Dii). Mouse NCs retain high viability in a sealed empty tube on ice, or room temperature for up to 1 h. Collect multiple levels of the NP as required into the same tube to

minimize variation of the digestion time (Figure 4F), and proceed to digestion of the tissue (Figure 4G,H). A freshly extracted mouse NP is observed as a clump of cells, but after 20 min digestion, are separated into single cells (Figure 4I,J). For larger IVD such as those from adult NCD dogs and pig IVDs, open the IVD space with a sterile no 22 blade at the border of

**TABLE 1** Digestion protocols.

Tissue type	Digestion enzymes	Resuspension medium
Mouse tissue	20 min in HBSS with 850 U/mL Collagenase II and 2.6 U/mL Dispase	HBSS +2% BSA
Rat tissue	30 min with 7 U/mL pronase followed by 4 h digestion with 125 U/mL collagenase type II	$\alpha$ MEM +1% P/S
Young dog tissue	1 h in $\alpha$ MEM with 37.5 U/mL collagenase type II	$\alpha$ MEM +1% P/S + 2% BSA
Adult dog tissue (NCD)	30 min in $\alpha$ MEM with 7 U/mL pronase followed by 4 h with 125 U/mL collagenase type II	$\alpha$ MEM +1% P/S
Pig tissue	30 min in $\alpha$ MEM with 7 U/mL pronase followed by 4 h digestion with 125 U/mL collagenase type II	$\alpha$ MEM +1% P/S
Fetal human tissue	30 min in $\alpha$ MEM with 37.5 U/mL collagenase type II	$\alpha$ MEM +1% P/S

Note: For mouse, young dog, and fetal human NP extraction enzymatic digestion with pronase, higher concentrations of collagenase, or longer digestion times considerably decreases NC viability and is not necessary because of the loose extracellular matrix. Collagenase (Worthington, LS004177), Dispase (Worthington, LS02109), and Pronase (11 459 643 001, Roche Diagnostics), are filtered with a 0.22  $\mu$ m membrane filter to ensure sterility, all incubations are performed at 37°C.

Abbreviations:  $\alpha$ MEM, alpha modified eagles media; BSA, bovine serum albumin; HBSS, Hanks buffered saline solution; NC, notochordal cell; NCD, nonchondrodystrophic; NP, nucleus pulposus; P/S, Penicillin/Streptomycin.

the cranial endplate. Distract the IVD space with the aid of a Hohmann retractor (approaching the spinal canal from the adjacent opened IVD). Collect the gel-like NP with the aid of a curette and transfer into a 50 mL tube with 10–15 mL alpha modified eagles media ( $\alpha$ MEM) +1% penicillin/Streptomycin (P/S).

## 2.4 | Recommendations for digestion of NP tissue and NC extraction

Following dissection, the NP tissue is placed in a 50 mL tube with 10–15 mL  $\alpha$ MEM +1% P/S, or 15 mL centrifuge tube for smaller discs (e.g., mouse) with 5 mL media. Centrifuge at 500 g for 5 min at room temperature (RT) and discard the supernatant. Of note is that contrary to degenerate NP tissue, NC-rich NP tissue is gel-like and generates a relatively loose pellet upon centrifugation requiring caution during removal of the supernatant. Incubate the collected NP tissue in digestion enzyme as per species specific methodology (Table 1). Place the tube on an orbital shaker at 37°C, 300 rpm during enzyme digestion. It is expected that after shorter term digestion periods, there will be a small number of remaining cell clumps, however, these can be readily dispersed by gently pipetting the cells with wide bore 1 mL tips. Centrifuge at 500 g for 5 min at RT and discard the supernatant. The expected outcome of this protocol is obtaining both single cells and clusters. Filter the sample over a 40- $\mu$ m cell strainer (the filtered solution will contain the nonclustered cells). Collect the NC clusters by washing the filter upside down with resuspension media (Table 1). After centrifugation at 500 g for 5 min, resuspend the cells in  $\alpha$ MEM with 1% P/S and count (see Numeration section). The <40- $\mu$ m fraction will contain single cells and smaller clusters, whereas the >40  $\mu$ m fraction will contain the larger clusters of predominantly NC-like cells with vacuoles, 25–85  $\mu$ m in diameter.

Of note, mouse NC digestion was particularly sensitive to digestion time, with an increase of digestion time from 20 to 30 min resulting in lower cell viability (Figure S1). Furthermore, the addition of 2% vol/vol bovine serum albumin in hanks buffered saline solution (HBSS)

during digestion improved cell viability compared with HBSS alone (Figure S1), which has also been found for puppy NC isolation, whilst this was not necessary for NC isolation from other species. A small study was conducted to compare harvested NCs from pig spines versus tail IVD which are often waste material from the meat industry. More NP tissue was extracted from pig spines than tail IVDs in line with the larger IVDs within the spine (Figure S2). However, no difference was observed in the total number of NCs harvested per disc (Figure S2) with greater number of NCs per gram of tissue in NP tissue taken from the smaller tail IVDs compared with larger spine IVDs. Furthermore, isolation from tails was experienced as simpler; IVD exposure was more straightforward than spines where collection is hampered by the facet joints and transverse processes. These results provide the opportunity to refine and reduce waste material, as tails can be sourced from waste material from the meat industry whilst the use of spines often wastes the associated meat joints, this is in line with 3Rs (replace, reduce, refine).<sup>69,70</sup>

## 2.5 | Digestion of whole IVD tissue where NP isolation is not possible (e.g., human fetal IVDs [<18 wpc])

The enzyme concentration and centrifugation steps reported in this section were designed to rapidly isolate cells and maximize the number of cells collected for RNA/protein extraction, thus further optimization may be required to ensure high cell viability (see section 2.4 as a guide).

Transfer the IVD to a petri dish containing PBS to remove blood cells from the sample, which may contaminate the collected NC population during FACS. Using fine forceps (scoop do not pinch), transfer the IVDs to 50 mL Falcon tube containing 15 mL 62.5 U/mL Collagenase Type II (Gibco<sup>®</sup>, 17 101–015) and 150 U/mL type I-S hyaluronidase (Sigma-Aldrich<sup>®</sup>, H3506) in  $\alpha$ MEM media containing 1% antibiotic/antimycotic solution. Incubate on an orbital shaker at 37°C for 2 h. Centrifuge at 500 g for 5 mins at RT and discard the

supernatant. Suspend the cell-pellet in a prewarmed nonenzymatic cell dissociation solution (e.g., Sigma, C1419) and incubate on the orbital shaker at 37°C for 10 min to help dissociate further cell aggregates. Centrifuge at 2000 g for 5 min at RT and discard the supernatant. Resuspend in 1 mL sterile PBS and pipette gently to disperse the pellet. Thereafter, the cells are strained to remove cell aggregates or debris that would interfere with downstream FACS with 50 µm cup type Filcon® (BD Biosciences, 340 629). The Filcon® cup is prewet with 500 µL PBS, before the application of the 1 mL cell suspension. Following washing with 500 µL PBS, the cell suspension is centrifuged at 500 g for 5 min at 4°C and FACS can be conducted as reported previously.<sup>45</sup> The notochordal population is typically 5%–20% of total viable cells (NC, AF, and CEP cells) from the digested IVD.<sup>45</sup>

## 2.6 | Calculating cell number

The characteristics of NCs contribute to creating an increasingly difficult cell type to count, due to the large cytoplasmic vacuoles, freshly isolated NCs range from 10 to 40 µm in diameter<sup>29,71</sup> and NCs exist as a network of large cell clusters, containing 10–400 cells<sup>64,72</sup>; with multiple tight cell-to-cell adhesions.<sup>73–75</sup> Furthermore, these large cell clusters are surrounded by a thin layer of matrix (notochordal sheath) which physically separates one cluster from another.<sup>73</sup> Whilst several techniques and specialist cell counters have been developed to count clusters of cells,<sup>76</sup> they often fail to accurately enumerate single cells. In order, to gain the most efficient and reliable cell count, the cell clusters must be dissociated.

The customary methods of dissociation include using enzymatic approaches, such as trypsin, TrypLE, dispase, and accutase<sup>49,77–82</sup>; and/or mechanical approaches, such as filters, chopping techniques, microfluidic devices, and various ways of pipetting.<sup>83</sup> Jager et al.<sup>83</sup> compared different ways of dissociating human induced pluripotent stem cells, which are grown in large clusters (17 000 µm<sup>2</sup>) if left untreated and therefore difficult to dissociate without cell loss.<sup>77</sup> They demonstrated that none of the mechanical methods of dissociation produced single cells or small cell clusters. Whereas the combination of TrypLE followed by trypsin/EDTA digestion produced dissociated samples where the individual cells could be easily distinguishable.<sup>83</sup>

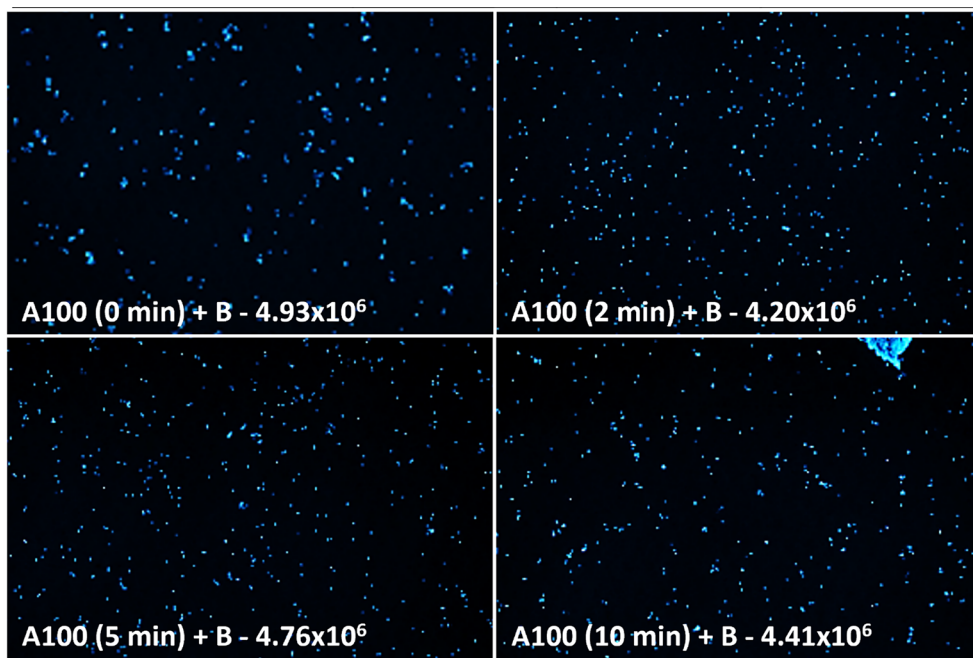
Within this study, enumeration methods were investigated to enable efficient and reliable dissociation of NC clusters which has not previously been reported. A comparison of dissociation methodologies was investigated to determine influence on cell count, viability, and resulting diameter, utilizing an automated cell counter (NucleoCounter® NC-200™ [Chemometec, Gydevang, Denmark]). Freshly extracted NC clusters were harvested from a single donor pig spine, as described above, and 500 µL of NC cell suspension in αMEM +1% P/S (allowing for triplicate repeats) was used to undergo different cell dissociation reagents. Dissociation reagents included either (a) solution 10 lysis buffer (Chemometec); (b) Solution A100 and B (Chemometec); (c) Accutase (Sigma); (d) Trypsin/EDTA (ThermoFisher, Gibco); (e) TrypLE (ThermoFisher, Gibco); and finally (f) TryLE followed by Trypsin. For solution 10 lysis buffer method; 100 µL NC

suspension was directly added to 100 µL solution 10 lysis buffer (Chemometec). The Solution A100 and B methods were conducted by taking 100 µL NC suspension sample and directly adding Solution A100 lysis buffer (Chemometec), leaving the NC sample in 100 µL solution A100 for 0, 2, 5, and 10 min, before next adding 100 µL of solution B stabilizing buffer (Chemometec). The Accutase method involved adding 1 mL of accutase (Sigma) directly to 100 µL of NC cell suspension, incubated for 10 min at 37°C, prior to being centrifuged for 1 min at 400 g and resuspended in 1 mL αMEM +1% P/S. Trypsin/EDTA method involved adding 1 mL of Trypsin/EDTA (ThermoFisher) directly to 100 µL of NC cell suspension, incubated for 10 min at 37°C, prior to being centrifuged for 1 min at 400 g and resuspended in 1 mL αMEM +1% P/S. Finally, TrypLE method also involved adding 1 mL of TrypLE (ThermoFisher) directly to 100 µL of NC cell suspension, incubated for 10 min at 37°C, prior to being centrifuged for 1 min at 400 g and resuspended in 1 mL αMEM +1% P/S. After dissociating NC suspension was counted using the NucleoCounter® NC-200™.

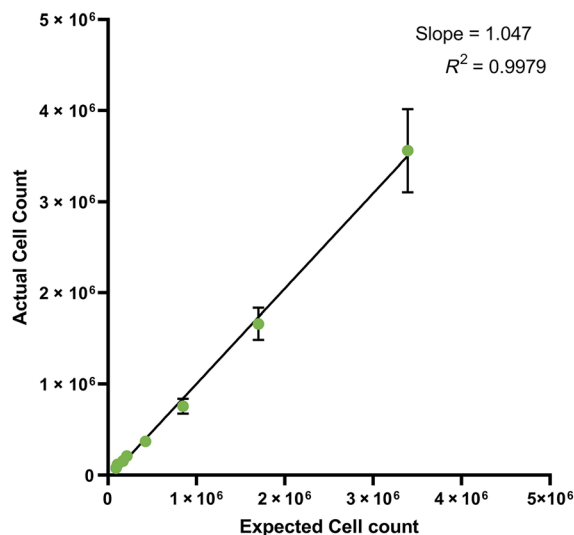
A combined analysis of images captured and the cell count (Figure S3) demonstrated that solution A100 and B could produce accurate cell counts and displayed visible NC dissociation, with the observation of single cells, whilst accutase, Trypsin, TrypLE, and TrypLE + trypsin resulted in reduced cell counts (Figure S3). Repeatability, linearity and range was further tested with the Solution A100 and B. The method of dissociating NC clusters with Solution A100 followed by the stabilizing solution B buffer after 2 min, showed the most promising method of dissociation (Figure 5). Prolonged incubation of NC clusters in solution A100 for more than 2 min caused the release of “sticky” DNA from neighboring dying cells causing the observation of cell clumps (Figure 5), whilst addition of solution A100 followed by immediate analysis (0 min) did not dissociate NCs into single cells (Figure 5). Linearity studies demonstrated excellent linearity with a slope of 1.047 and R2 of 0.9979 compared with expected cell number (Figure 5). Thus, the recommended methodology for numeration is to add 100 µL of solution A100 lysis buffer (Chemometec) to 100 µL of cell suspension, and incubate for 2 min at RT. Following incubation 100 µL of stabilizing buffer (Solution B [Chemometec]) should be added. The resulting cell suspension with solution A100 and B is then loaded into the Via1-Cassette™ (Chemometec) and read with the NucleoCounter® NC-200™ to provide a NC count allowing for the 1 in 3 dilution of the original cell suspension due to addition of 1:1:1 cell suspension, Solution A100, and Solution B. If a NucleoCounter® is not available we would recommend following the dissociation method described above and proceed to simple cell count using a manual hemocytometer, whilst automatic counting decreases subjective counting and user error and increases throughput.

## 3 | CRYOPRESERVATION OF NCS

Cryopreservation of NCs in the presence of a cryoprotective agent comes with anecdotal challenges in achieving a high cell viability after thawing. During freezing, the intracellular water molecules can form



**FIGURE 5** Numeration methodology for notochordal cells (NCs) using Chemometec nucleocounter. Dissociation of NCs was performed using solution A100 lysis buffer for 0, 2, 5, or 10 min prior to addition of Solution B stabilizing buffer. Similar total cell counts were observed; however, at 0 min cell clusters were still present and if A100 was left on for 10 min larger clumps could be visualized. Thus, a 2-min incubation time was selected for further linearity testing. Linearity studies comparing expected cell number via serial dilution was confirmed with a slope of 1.047 and  $R^2$  of 0.9979.



ice crystals which can damage cell membranes and other organelles and result in cell death. Cryoprotective agents prevent the formation of these ice crystals,<sup>84</sup> nonetheless the effectiveness therefore may depend on the cell type. Mature NPCs have been shown to maintain high viability after cryopreservation with the use of dimethylsulfoxide (DMSO) and fetal calf serum (FCS) as cryoprotective agents,<sup>85,86</sup> and is the most utilized methodology in the spine field.<sup>87</sup> Yet, there is little information on the cryopreservation of NCs. One of the key challenges relates to the NC vacuoles thought to contain a high-water content making NCs more susceptible to the formation of ice crystals in comparison to nonvacuolated NPCs.<sup>88</sup> In addition, NCs are present in cell clusters, which could prevent the cryoprotective agents from entering cells within the center of large cell clusters.

To determine whether NCs could be cryopreserved and the optimal method to maintain viability and phenotype, different types and concentrations of cryoprotective agents were examined. The NCs were extracted from 10-week-old pig spines ( $n = 3$ ) and

cryopreserved in (a) 20% vol/vol FCS in  $\alpha$ MEM with different percentages of DMSO (0%, 5%, 10%, or 20%), (b) 10% glycerol +90% FCS, or (c) using a commercially available cryoprotective agent: CryoStor<sup>®</sup> CS10 (07930, Stemcell Technologies). Freshly isolated NCs were cryopreserved in a precooled (4°C) Mr. Frosty<sup>™</sup> freezing container which was put in  $-80^{\circ}\text{C}$  overnight. Sixteen hours thereafter, the NCs were transferred to liquid nitrogen ( $-196^{\circ}\text{C}$ ). After 1 week, the NCs were thawed in a water bath ( $37^{\circ}\text{C}$ ) and the number and viability of the NCs were determined using the NucleoCounter<sup>®</sup> NC-200<sup>™</sup>.

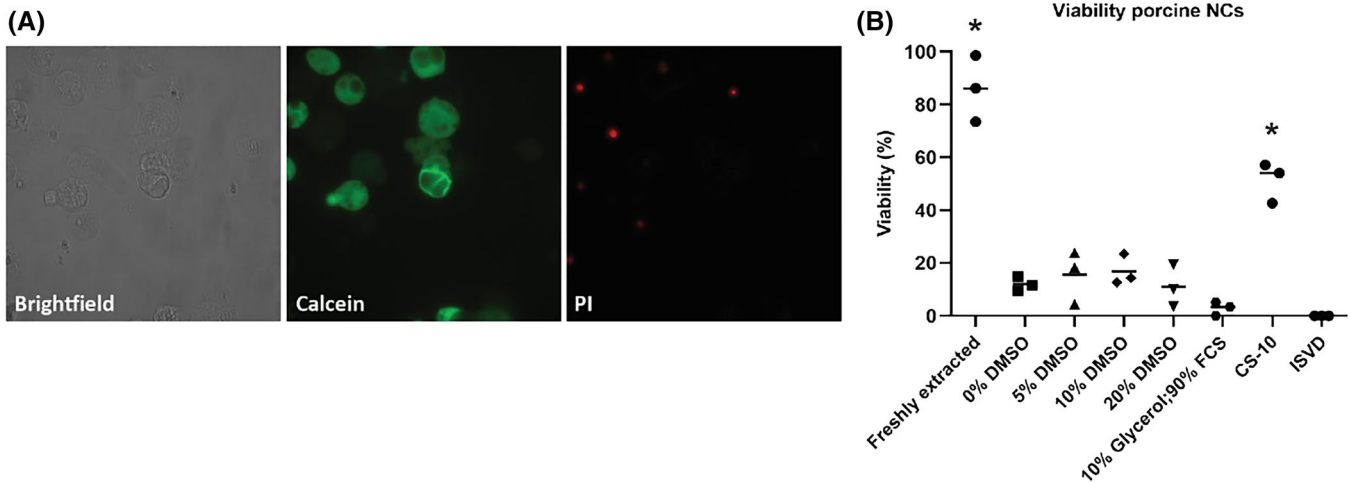
Since NCs can be compared with oocytes because of their large size and high-water content and oocytes are successfully cryopreserved with in-straw vitrification-dilution (ISVD), this method was also tested for NC cryopreservation. Straws were prepared as described by Inaba et al.,<sup>89</sup> As handling medium,  $\alpha$ MEM was used and as a diluent solution  $\alpha$ MEM +0.5 M sucrose. Both single NCs (<40  $\mu\text{m}$  fraction) and clusters (>40  $\mu\text{m}$  fraction) were resuspended in 1.6 M ethylene glycol and incubated for 5–15 min at RT to adjust to the



isotonic volume. After centrifugation, the cells were resuspended in 75  $\mu$ L vitrification solution (1 M sucrose +10% glycerol in  $\alpha$ MEM).<sup>90</sup> Three times 25  $\mu$ L cell suspension was taken up per straw, whereafter the straws were sealed using a heat-sealing machine. The straws were frozen directly in liquid nitrogen and stored at  $-196^{\circ}\text{C}$ . The ISVD straws were thawed by holding them in the air for 5 s, whereafter they were swirled in a water bath ( $37^{\circ}\text{C}$ , 8 s). The straws were placed in a vertical position for 1 min to mix the different contents, whereafter they were placed horizontally for 5 min to allow the cells to

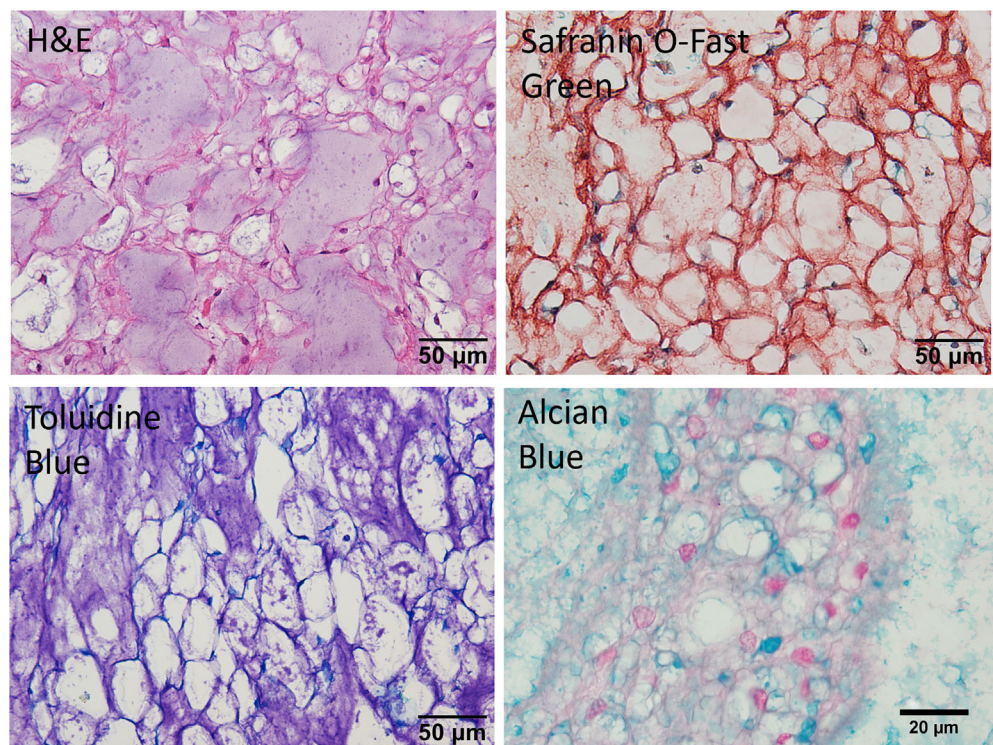
calibrate to their osmotic environment and temperature. Next, the sealed parts were cut off and the cells were transferred to empty tubes. After centrifugation (500 g, 5 min) cell viability was assessed using the NucleoCounter<sup>®</sup> NC-200™.

The viability of the NCs directly after extraction was high (>70%) (Figure 6), however, following cryopreservation low viability levels were seen (between 5% and 20% in all the different concentrations of DMSO and the 10% glycerol +90% FCS solution; Figure 6). IVSD cryopreservation failed to yield viable NCs after thawing.



**FIGURE 6** Viability of porcine notochordal cells (NCs) following cryopreservation testing: (A) Brightfield and Calcein-AM and propidium iodide (PI) staining images of freshly extracted porcine NCs. (B) Viability of NCs directly after extraction, after cryopreservation using different methods ( $n = 3$  donors). \* $p < 0.05$  from all other conditions except condition with same symbol. Statistics performed with IBM SPSS statistics, Mann-Whitney  $U$  test, corrected for multiple comparisons (Benjamini-Hochberg post hoc test). ISVD, in-straw vitrification-dilution.

**FIGURE 7** Histological appearance of notochordal cell (NC) rich pig disc: NCs can be visualized clearly within a rich matrix of collagens and proteoglycans. NCs can be seen in large clusters of cells and display a vacuolated morphology. Which can be visualized with a variety of histology stains including hematoxylin and eosin (H&E), Safranin O-Fast green, Toluidine Blue, and Alcian Blue-Picrosirius Red.



**TABLE 2** Detection of key phenotypic markers in the embryonic notochord cells (eNC), notochordal cells (NCs), and the nonvacuolated nucleus pulposus cells (NPCs).







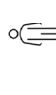
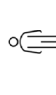









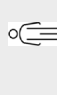


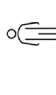


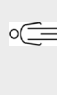







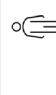












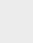

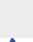
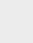

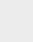


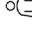
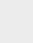







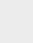





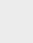






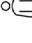
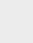






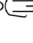
Marker gene	Description	eNC	NC	NPC	References
TBXT (T, Brachyury)	T-Box Transcription Factor T. Involved in the transcriptional regulation of genes required for mesoderm formation and differentiation				19,44,71,91-94
CAV1	Caveolin-1. Acts as a scaffolding protein within caveolar membranes				95-97
CD24	Cluster of differentiation 24. Cell surface sialoglycoprotein expressed at the surface of immune as well as epithelial, neural, and muscle cells				19,44
DSTYK/RIPK5	Dual serine/threonine and tyrosine protein kinase. NC Sheath protein				98
FOXA2	Forkhead box protein A2. Transcription factor involved in embryonic development, establishment of tissue-specific gene expression and regulation of gene expression in differentiated tissues				92
FOXF1	Transcription factor involved in embryonic development, establishment of tissue-specific gene expression and regulation of gene expression in differentiated tissues				19,99,100
FOXJ1	Forkhead Box J1. Transcription factor specifically required for the formation of motile cilia				101
KRT18	Keratin 18. Encodes the type I intermediate filament chain				19,34,44
KRT19	Keratin 19. Smallest known acidic cytokeratin specifically expressed in the periderm, the transiently superficial layer that envelopes the developing epidermis				19,44,91
LGALS3	Galectin 3. Encodes advanced Glycation End-Product Receptor				19,34,44,102
NOG	Noggin. Inhibitor of bone morphogenetic proteins (BMP) signaling which is required for growth and patterning of the neural tube and somite				103
NOTO	Notochord homeobox. Transcription regulator acting downstream of both FOXA2 and Brachyury during notochord development				13,92,104
SHH	Sonic Hedgehog Signaling Molecule. Encodes a protein that is instrumental in patterning the early embryo				42,91,92,103,105
SOX-5	SRY-Box Transcription Factor 5. Involved in the regulation of embryonic development and in the determination of the cell fate				17,106

TABLE 2 (Continued)

Marker gene	Description	eNC	NC	NPC	References
SOX-6	SRY-Box Transcription Factor 6. Involved in several developmental processes, including neurogenesis, chondrocytes differentiation and cartilage formation				17,106
SOX-9	SRY-Box Transcription Factor 9. Transcription factor involved in chondrocytes differentiation and skeletal development		 		92,106–111
ACAN	Aggrecan. Major proteoglycan component of the IVD extracellular matrix		 		42,75,102,110,112–114
AQP-6	Aquaporin 6. Encodes for a membrane proteins that functions as a water channel in cells. Shown to clearly highlight vacuoles in NCs	 	 	 	71
CA12	Carbonic Anhydrase 12. Member of the large family of zinc metalloenzymes that catalyze the reversible hydration of carbon dioxide				19
CDH2 (CD325, N-CADHERIN)	Cadherin 2. Encoded preproprotein is proteolytically processed to generate a calcium-dependent cell adhesion molecule which plays a role in the establishment of left–right asymmetry, development of the nervous system and the formation of cartilage and bone		 		94,115
COL2A1 and COL2A2	Collagen Type II Alpha 1 Chain and Collagen Type II Alpha 2 Chain		  		33,42,94,110,116
COL6A1	Collagen Type VI Alpha 1 Chain		 		32,42,113,117–119
GJA1 (CX43, Connexin-43)	Gap Junction Protein Alpha 1. Encoded protein is a component of gap junctions, which are composed of arrays of intercellular channels that provide a route for the diffusion of low molecular weight materials from cell to cell				112,115
GLUT-1 (SLC2A1)	Glucose Transporter Type 1/ Solute Carrier Family 2 Member 1. Encodes a major glucose transporter				120–122
HIF-1 $\alpha$	Hypoxia-inducible factor 1-alpha. Regulates genes that enable cell survival in a hypoxic environment, including those involved in glycolysis, angiogenesis, and expression of growth factors	 	 		99,121
KRT8	Keratin 8. Typically dimerizes with keratin 18 to form an intermediate filament in simple single-layered epithelial cells. Plays a role in maintaining cellular structural integrity and also functions in signal transduction and cellular differentiation		 		13,19
PAX-1	Paired Box 1. Involved in pattern formation during embryogenesis and may be essential for development of the vertebral column		 		19,99,106,108

(Continues)

TABLE 2 (Continued)

Marker gene	Description	eNC	NC	NPC	References
TEK (TIE2)	TEK Receptor Tyrosine Kinase. Encodes a protein that acts as cell-surface receptor for ANGPT1, ANGPT2 and ANGPT4. Regulates angiogenesis, endothelial cell survival, proliferation, migration, adhesion and cell spreading, reorganization of the Actin cytoskeleton, but also maintenance of vascular quiescence				123–125

Note: Evidence for expression identified at protein level based on immunostains, reporter expression, mass spectrometry or FACS. Confirmed protein expression is indicated for the cells residing within the notochord (eNCs) and the core of the intervertebral disc (NCs and NPCs). Within individual species: zebrafish; nonchondrocytic dog; pig; cow; human; rat;

dog; pig; cow; human. Blue icons indicate examples presented in the current article (Figures 8 and 9). Note that immunopositivity is largely dependent on the antibodies employed and tissue processing methods and the absence of expression may indicate a lack of data and technical difficulties in protein detection. In the absence of protein expression data, evidence from in situ hybridization indicates the localization of gene expression in their cellular environment (Boxed symbols). Gene descriptions refer to data from <https://www.genecards.org/>.

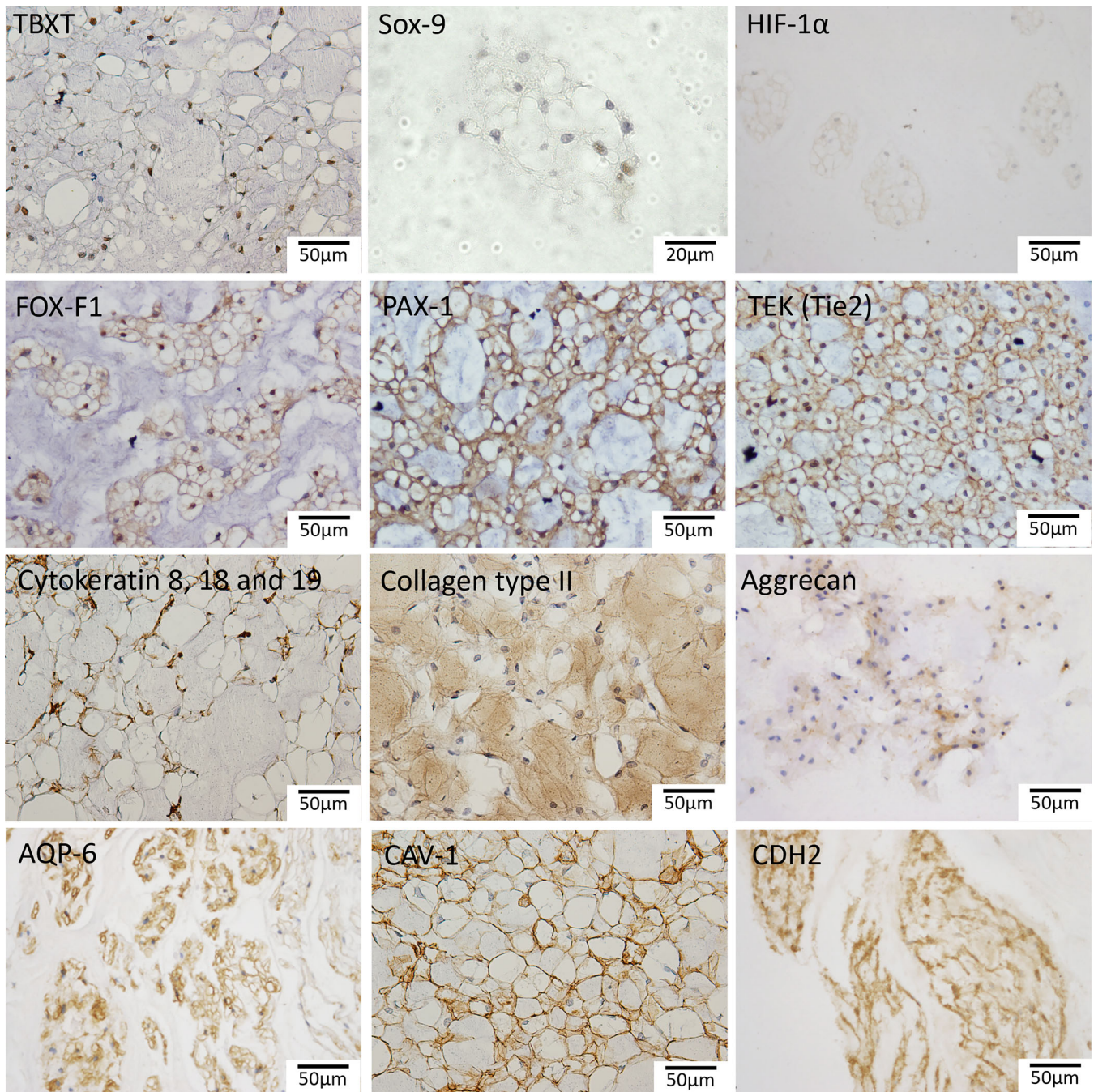
Interestingly, NCs cryopreserved in CS-10 had a much higher viability (50%–60%) than the NCs cryopreserved in all other cryoprotective agents (Figure 6). In conclusion, to date, all tested cryopreservation methods resulted in large loss in NC viability. CS-10 showed highest viability levels with only 50% NCs remaining viable, but as a commercial product the content of this solution is unknown and further work would be required to determine phenotype following cryopreservation. It is thus currently recommended that NCs are utilized directly from extraction and not cryopreserved.

### 3.1 | Characterizing the phenotype of NCs

Characterization of the phenotype of NCs residing in the IVD is essential to understand whether this phenotype can be maintained during culture. The morphological appearance of NCs, in particular the large vacuolated NCs, are distinctive and can be identified via numerous histological stains as described previously<sup>68</sup> and showcased in Figure 7.

Here, we describe potential markers which can be useful to investigate key phenotypic and functional features of NCs, and whilst these are not all specific to NC phenotype, together they form a picture of cell status (Table 2).<sup>13,17,19,32–34,42,44,71,75,91–125</sup> Cells that reside within the NP experience dynamic changes of gene transcription profiles throughout postnatal cell proliferation, differentiation, IVD growth, aging, and degeneration. The recent review by Bach et al.,<sup>15</sup> discussed potential markers which can be utilized to aid in the characterization of eNCs, NCs to NPCs highlighting key issues with identification of NC/NP-specific markers and differential results between studies. Whilst a number of key markers have been suggested to identify NC and NPCs, the evidence for NC-specific markers is currently lacking, with cross expression across multiple cell types (Table 2). Expression of certain previously proposed NP markers (SHH, TBXT, KRT18/19, CA12, CD24, HIF-1 $\alpha$ , GLUT-1)<sup>40</sup> are lost in older mature NPCs and hence could be useful to separate NCs from mature NPCs. Considering that the NC-rich NP can be properly isolated, the use of these markers is not complicated by the fact that they are also expressed by other similar cell types such as articular chondrocytes.<sup>99</sup> Interestingly many markers which have been described have not yet been investigated at protein level within most/any species, demonstrating a need for further characterization (Table 2).

In this context, key factors involved in normal NC physiology provide useful functional characterization markers for NCs (Table 2). Furthermore, NCs are distinguished from the smaller mature NPCs by the presence of vacuoles and the formation of large cell clusters, which are surrounded by a rich ECM NC sheath and thus key markers for these characteristics could be useful additional factors. Although cellular clusters are also observed during human disc degeneration,<sup>126–129</sup> and thus additional markers in addition to clustering are essential to separate the juvenile NC and a cluster of NPCs from degenerate discs. The NC vacuoles express high levels of aquaporins (AQP) on the membrane,<sup>71</sup> with AQP-6 demonstrating high intensity, which could be utilized to aid in vacuole identification (Figure 8). Dual serine/threonine

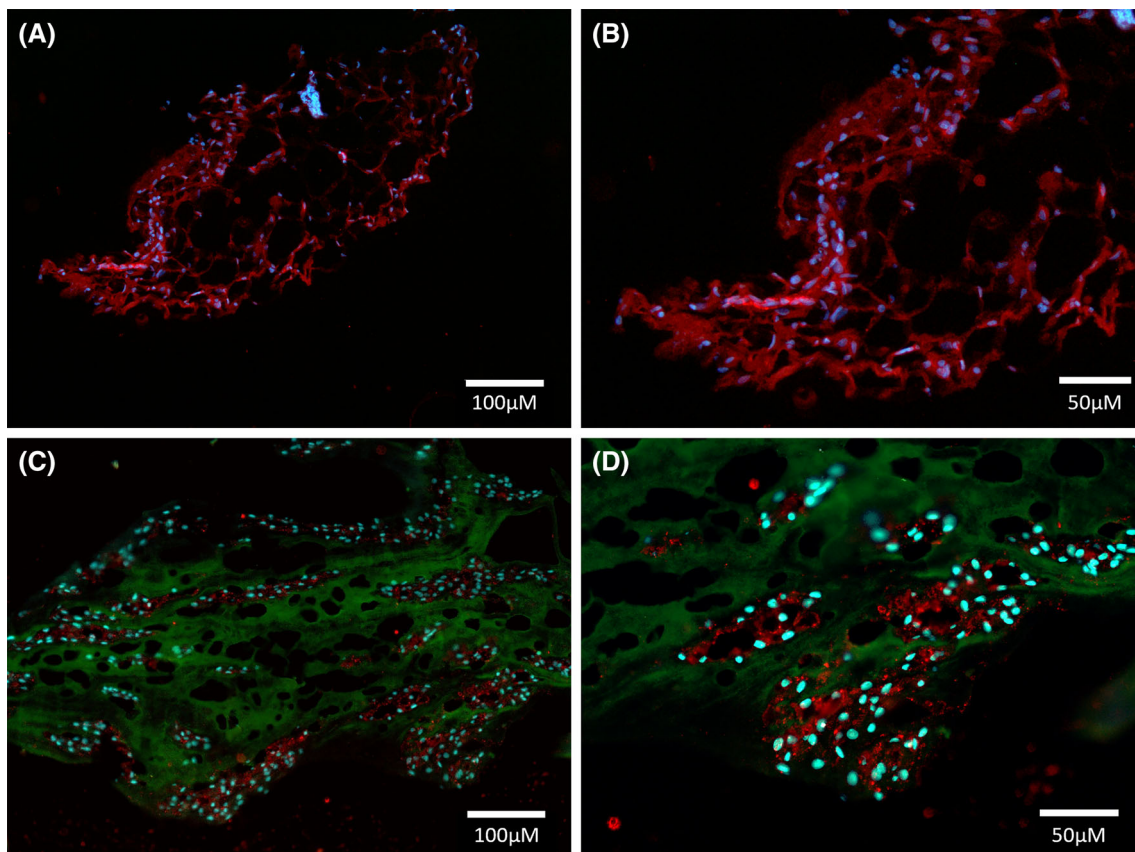


**FIGURE 8** Immunohistochemical staining of notochordal cell (NC) rich pig and dog nucleus pulposus (NP) tissue: Immunohistochemistry was utilized to identify localization for potential characterization markers of NCs. TBXT, SOX9, HIF-1 $\alpha$ , FOXF1, PAX-1, TEK (Tie 2), Pan Cytokeratin (8,18,19) Collagen type II, Aggrecan, CAV-1, and CDH2 were all observed within the NC rich regions of the NP of pig discs. AQP-6 staining was shown for dog discs. Scale bars = 50  $\mu$ m except for SOX9 which is shown at higher magnification and 20  $\mu$ m scale bar.

and tyrosine protein kinase (DSTYK) also known as receptor interacting protein 5 (RIPK5) is required for notochord vacuole biogenesis and integrity, DSTYK mutants in zebrafish causes scoliosis-like phenotype in fish, and overexpression leads to vacuole formation in sheath cells.<sup>98,130-134</sup> To date, limited studies have investigated the presence or role of RIPK5 within mammalian NCs, and therefore, its expression is investigated here within 3-month-old pig NCs. RIPK5 was identified

within porcine NCs, mainly around large NC clusters and thus could be a useful additional marker of NCs (Figure 9).

The “large NC clusters” are supported by multiple cell adhesion molecules, including gap junction proteins and cadherins. The presence of functional gap junctions anchored to the actin cytoskeleton, specifically connexin-43, has been shown in NC clusters from NCD dog NP.<sup>73,74</sup> Furthermore, cadherins which are membrane-spanning



**FIGURE 9** Immunofluorescence staining for notochordal cell (NC) rich pig NP tissue. Immunofluorescence staining for DSKY-5 (A,B), and costaining for AQP-6 (red) and collagen type II (green) (C,D). Scale bar as stated 100 or 50  $\mu\text{m}$ .

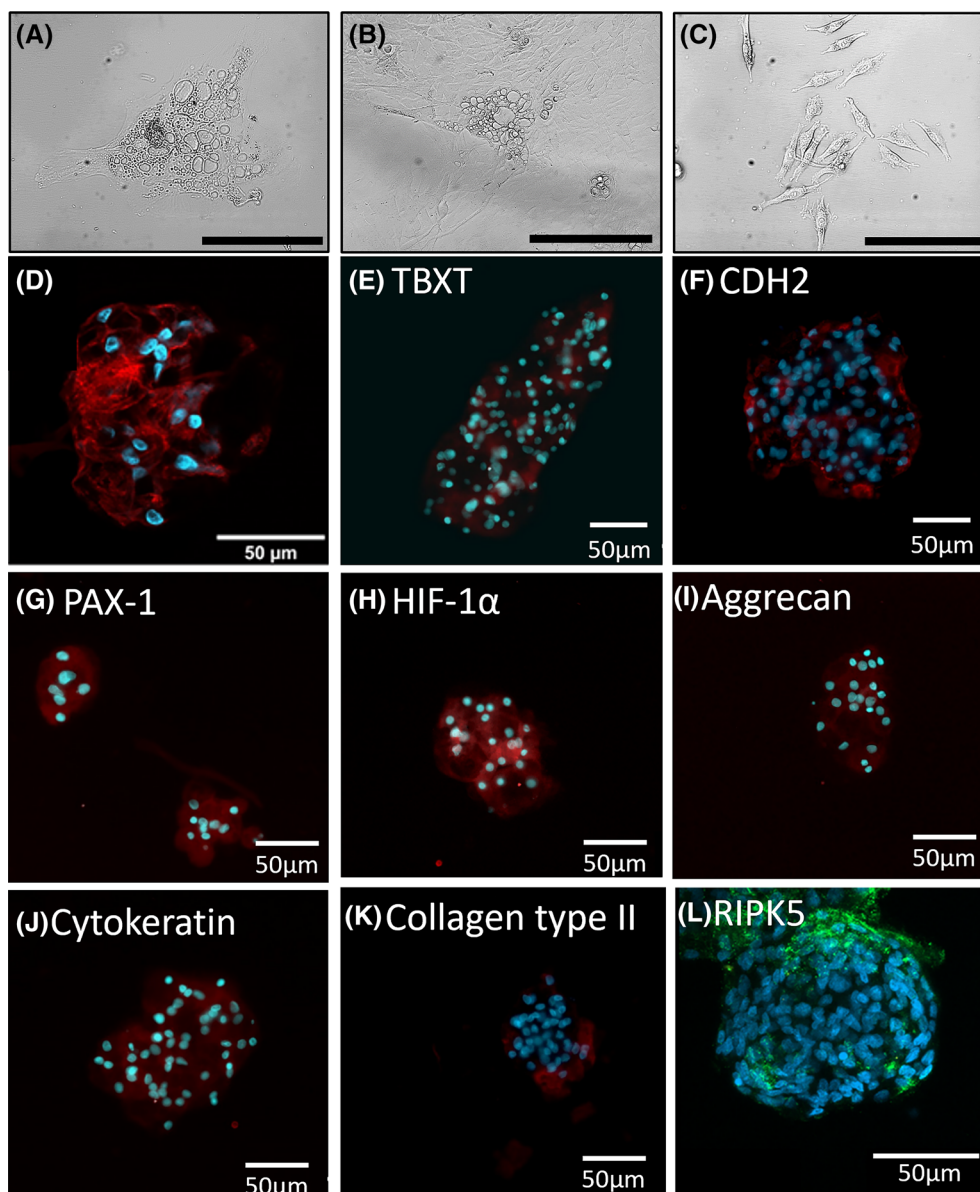
macromolecular complexes responsible for cell–cell adhesion,<sup>75,135</sup> regulate the stability and cell contact formation. NC-rich NP tissues, including juvenile human discs and other animals, express high levels of CDH2(N-cadherin, CD325) with a decrease in CDH2 correlating with the disappearance of cell clustering during aging, as NCs are replaced by widely separated NPCs. Microarray and immunostaining have also implicated the membrane protein CAV1 (caveolin 1), an essential regulator of cell adhesion and migration, and is decreased during differentiation of NC to NPCs<sup>52,95</sup> and associated with progression of degeneration.<sup>95</sup>

The “NC sheath” has been shown to be highly important in the homeostasis of the developing spine within zebrafish, with scarce studies investigating this in mammals. The NC sheath is responsible for segmental patterning of the spine.<sup>11,130</sup> Structurally, the NC sheath is composed of three different layers that are comprised of laminin, fibrillin, fibronectin, proteoglycan, and collagen.<sup>134</sup> Studies that used zebrafish deficient in  $\alpha 1\alpha 4$  or  $\alpha 1\alpha 5$  chain of laminin,<sup>131</sup> the B1 and  $\gamma 1$  chains of laminin-1,<sup>134</sup> Emilin-3,<sup>132</sup> Collagen 8<sup>133</sup> and Collagen 9 $\alpha 2$ <sup>98,130</sup> disrupt the sheath layer leading to a kinked spine and less vacuoles in NCs, which has also been linked to RIPK5 expression.

As a showcase, immunohistochemistry was utilized to determine the expression and localization of key proposed NC/NPC phenotypic markers within the NC-rich pig disc. Freshly extracted discs of juvenile pigs were formalin fixed and paraffin embedded, 4  $\mu\text{m}$  sections were

utilized for IHC (Table S1) using previously published IHC protocols.<sup>136</sup> NP tissue within the NC-rich pig discs were shown to express positive immunohistochemical staining for a number of potential NC markers including TBXT, SOX-9, HIF-1 $\alpha$ , FOX-F1, PAX-1, TIE-2, and pan-cytokeratin (Figure 8). Furthermore, ECM markers collagen type II and aggrecan were identified both within the ECM and cellular expression (Figure 8). Vacuoles within NCs could be clearly seen using both AQP-6 and CAV1 markers (Figure 8), whilst CDH2 was also highly expressed (Figure 8). Immunofluorescence was also utilized to identify expression of DSTYK/RIPK5 within native porcine discs and was shown to be highly expressed by NCs, particularly located around large NC clusters (Figure 9), in a similar pattern to the NC sheath seen in zebrafish. Immunofluorescence also enables co-staining of cell and ECM markers, with the showcase demonstrated for AQP-6 and COL2 (Figure 9).

In conclusion, the characterization of NC-specific markers, conserved across species and of physiological relevance, that can be utilized to define stage-specific cell types found in the notochord and later in the NP from eNCs to NCs and then NPC is still subject to discussion by experts in the field and remains to be fully resolved (see review Bach et al.,<sup>15</sup>). Advances in “omic” technologies and in particular single cell or spatial profiling approaches hold promise to enable NC marker discovery and improve characterizing and benchmarking the NC and NPCs phenotypic changes across species during their life

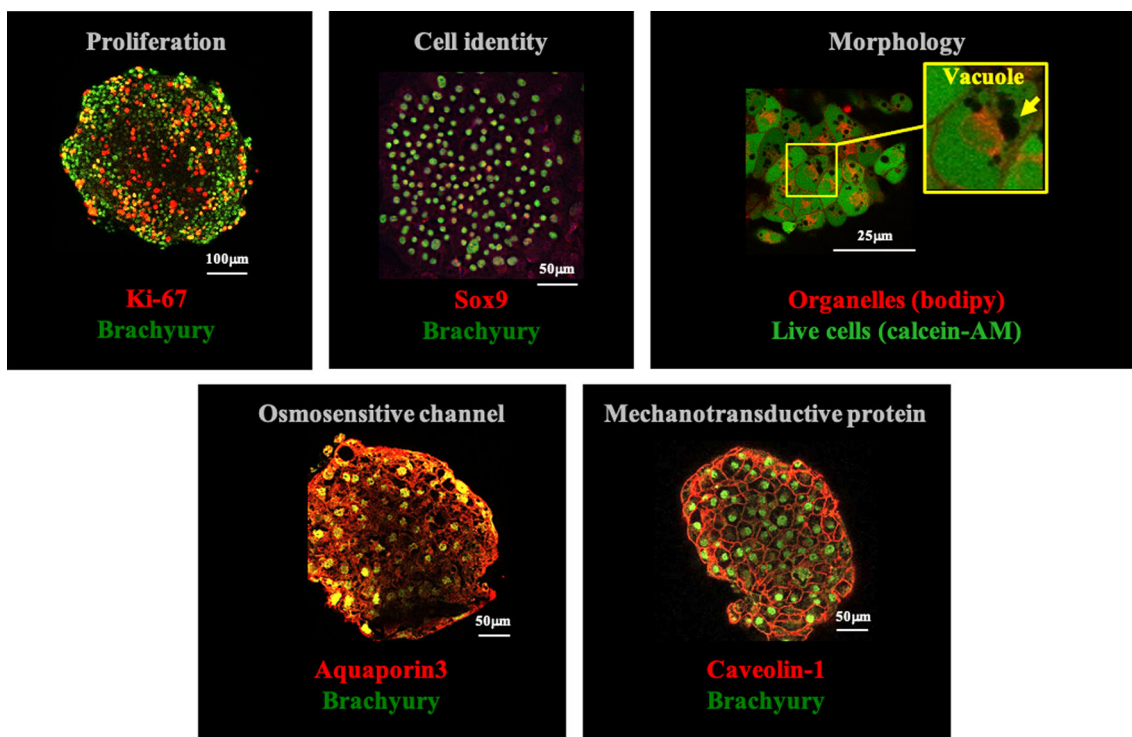


**FIGURE 10** Notochordal cell (NC) morphology and phenotype within in vitro culture. (A–C) Monolayer culture and morphology of cells directly extracted from rat nucleus pulposus tissue. (A) Clusters of large, vacuolated NCs are the main cell type present during 2D in vitro culture 1 day after extraction from rat nucleus pulposus (NP) tissue, although some smaller, nonvacuolated cells are also present. (B) After 7 days in 2D in vitro culture, the number of clustered, vacuolated cells has reduced, whereas the number of smaller, nonvacuolated cells has increased. The remaining clusters of vacuolated cells are surrounded by smaller, nonvacuolated cells. (C) At 10 days postextraction, the clusters of large, vacuolated cells have almost completely been replaced by or differentiated into smaller, nonvacuolated cells. Scale bar 50  $\mu$ m. (D) Rat NCs cultured in alginate in 400 mOSM/L  $\alpha$ MEM maintained clusters and vacuolated morphology as shown by Phalloidin and DAPI staining following 1 day in culture. (E–L) Immunofluorescence staining for NC characterization markers in rat NCs cultured in alginate for 4 days. (E) TBXT, (F) CDH2, (G) PAX-1, (H) HIF-1 $\alpha$ , (I) Aggrecan, (J) Pan Cytokeratin (8,9,19), (K) Collagen type II. (L) DSKY-5 immunofluorescence staining in porcine NCs cultured in alginate for 14 days. Scale bars = 50  $\mu$ m.

journey.<sup>42,43</sup> Based on current knowledge particularly evidence from immunopositivity and the expression profile of potential markers which can be deployed to characterize NCs (Table 2 and Figures 8 and 9). However, given that many of the markers are expressed through eNCs, NCs, and NPCs to discriminate between these cell types and to evidence NC phenotype coexpression at the level of single cells should be aimed using techniques such as coimmunostaining analysis.

### 3.2 | Cell expansion and culture whilst maintaining phenotype

The expansion and culture of freshly isolated vacuolated NCs, whilst also maintaining their in vivo-like phenotype, remains challenging. If cultured within a standard monolayer system, NCs rapidly lose their clustered, vacuolated phenotype between 6 and 28 days or between



**FIGURE 11** Micromass culture of mouse notochordal cell (NC) Immunofluorescence co-localization: Immunofluorescence images showing Ki-67+/Brachyury+ proliferative NCs, coexpressing SOX9+/Brachyury+, AQUAPORIN3+/Brachyury+, and Caveolin-1+/Brachyury+ NC-specific markers, respectively and showing vacuoles within the cytoplasm where the calcein-AM fluorophore is excluded (yellow arrowhead).

1 and 3 passages, and present morphologically as smaller, singular, nonvacuolated cells (Figure 10), a phenomenon reported across multiple species.<sup>52,55,58,66</sup> During this change in morphology, it has been observed that the expression of NC markers TBXT, KRT8/19, is decreased indicating that the smaller, nonvacuolated cells are phenotypically distinct from the originally extracted vacuolated NCs.<sup>55,58</sup> In addition, vacuolated cells are quickly outcompeted by small, nonvacuolated cells in monolayer culture, as their growth rate is significantly slower.<sup>55,65</sup>

Therefore, specialized techniques have been developed which utilize several environmental cues, for the retention of the vacuolated NC phenotype during in vitro culture and expansion. It has been well established that 3D alginate bead culture helps to maintain the in vivo phenotype of mature nonvacuolated cells.<sup>67</sup> When vacuolated cells are cultured within alginate beads viability and culture duration were increased, their clustered, vacuolated morphology was retained, when compared with monolayer culture, with most studies to date using  $\alpha$ MEM media.<sup>55,57,59,65</sup> This indicates 3D alginate bead culture is an appropriate method that enables retention of native phenotype. In addition, alginate bead culture under physioxenic (2%  $pO_2$ )<sup>55</sup> and physiological osmolarity (400 mOsm/L in  $\alpha$ MEM media),<sup>64</sup> increased vacuolated cell marker expression and clustering. Furthermore, there is evidence that the vacuolated cell phenotype can be retained under specific culture conditions in vitro. Initial short-term alginate culture caused some loss of phenotype, yet this was restored after 28 days in culture, indicating the initial NC vacuolated

phenotype may be lost after isolation, but then at least partially recovered following extended 3D culture under appropriate osmotic culture conditions.<sup>64</sup>

3D culture systems such as alginate fail to enable expansion of NCs, thus alternative substrate surfaces together with environmental conditions have been investigated in the attempt to maintain phenotype whilst enabling expansion. Humphreys et al.,<sup>137</sup> investigated retention of the vacuolated cell phenotype of pig NCs in 2D culture, with the use of cell culture substrate coatings, oxygen concentration, osmolarity, and surface stiffness. The greatest levels of cell adhesion and proliferation, morphology, and expression of NC phenotypic markers (CD24, KRT8, KRT18, KRT19, and TBXT) were observed with the use of laminin-521-coated surfaces with 0.5 kPa stiffness and  $\alpha$ MEM media, under 2%  $pO_2$ , 400 mOsm/kg culture conditions, where highest number of vacuolated NC cells (around 70%) were retained.<sup>137</sup> This indicates that the vacuolated NC phenotype can also be maintained under specific 2D culture conditions, where at least some population doubling is possible.<sup>137</sup> However, culture within such conditions can be difficult to obtain across laboratories and thus where proliferation of NCs is not required we recommend that clusters of isolated NCs are maintained as clusters and cultured within alginate beads in  $\alpha$ MEM media, under physiological  $O_2$  concentration (1%–5%) and osmolarity (400 mOsm/L), in FCS free media such as that described for alginate culture of NPCs with the inclusion of insulin-transferrin-selenium, Albumax and L-Proline,<sup>87</sup> as this enables the retention of their in vivo morphology



(Figure 10) and maintained the expression of NC phenotypic markers, including TBXT, CDH2, PAX1, HIF-1 $\alpha$ , pan KRT, COL2, ACAN, AQP-6, and RIPK5 (Figure 10).

Recent micromass cultures have also been investigated for a simple and reproducible 3D culture model of NCs, to study basic biology and function, isolated from mouse immature NP tissue.<sup>97</sup> Culture conditions were optimized to enable growth of self-organized micro-masses of NCs in suspension. This 3D model system successfully preserves the phenotype of mouse NCs, which was determined by maintenance of the intracytoplasmic vacuoles, the expression of NC characteristic markers (TBXT; SOX9) and the synthesis of proteins related to their function (CAV1; AQP3; Figure 11). However, this remains to be confirmed for other species and mature NCs.

## 4 | CONCLUSIONS

This article aims to provide key recommendations for the extraction of NCs from multiple species from mice to humans. Providing tips and tricks to harvest maximal viable cells to enable downstream studies and analysis with differential methodology particularly for fetal tissues. Considerations for numeration of NCs are provided with a recommended methodology which enables accurate counting despite the challenges of the tight NC clusters. The issues associated with cryopreservation of these cells are discussed and further work is required to identify whether these cells can be cryopreserved. Recommendations are provided for NC characterization: whilst to date no marker is specific to NCs, by utilizing a phenotypic panel approach their characterization is possible. New insights in phenotypic markers using single-cell transcriptomics, which many groups are currently working on, will in the future provide for improved characterization methodologies to further understand these fascinating cells. Together we hope that this article will provide a road map for in vitro studies using NCs derived from a range of commonly utilized species, which can enable acceleration of research.

### AUTHOR CONTRIBUTIONS

Anne Camus, Marianna A. Tryfonidou, and Christine L. Le Maitre, contributed to conception of the study. Rebecca J. Williams, Lisanne T. Laagland, Frances C. Bach, Anne Camus, Marianna A. Tryfonidou, and Christine L. Le Maitre, contributed to the design of the study. Rebecca J. Williams, Lisanne T. Laagland, Frances C. Bach, Lizzy Ward, Shaghayegh Basatvat, Wilson Chan, Joseph W. Snuggs, and Lily Paillat contributed to acquisition of laboratory data (Rebecca J. Williams: Porcine and Rat isolation, numeration studies, characterization, and culture; Lisanne T. Laagland: Canine and porcine isolation and characterization; Frances C. Bach: human, canine, and porcine isolation; Lizzy Ward: human isolation; Shaghayegh Basatvat: porcine isolation; Wilson Chan: mouse isolation; Joseph W. Snuggs: rat isolation, monolayer culture, and characterization; Lily Paillat: mouse isolation). Rebecca J. Williams, Lisanne T. Laagland, Frances C. Bach, Shaghayegh Basatvat, Stephen

M. Richardson, Wilson Chan, Joseph W. Snuggs, Lily Paillat, Marianna A. Tryfonidou, and Christine L. Le Maitre performed data analysis. Rebecca J. Williams, Lisanne T. Laagland, Frances C. Bach, Lizzy Ward, Wilson Chan, Vivian Tam, Adel Medzikovic, Lily Paillat, Joseph W. Snuggs, Deepani W. Poramba-Liyanage, Judith A. Hoyland, Danny Chan, Anne Camus, Stephen M. Richardson, Marianna A. Tryfonidou, and Christine L. Le Maitre contributed to interpretation of the data. Rebecca J. Williams, Lisanne T. Laagland, Frances C. Bach, Lizzy Ward, Wilson Chan, Vivian Tam, Adel Medzikovic, Shaghayegh Basatvat, Nicolas Vedrenne, Joseph W. Snuggs, Deepani W. Poramba-Liyanage, Danny Chan, Anne Camus, Marianna A. Tryfonidou, and Christine L. Le Maitre drafted the article. All authors critically revised the article for intellectual content. All authors approved the final version and agree to be accountable for all aspects of the work.

### ACKNOWLEDGMENTS

This publication has received funding from the European Union's Horizon 2020 research and innovation program (iPSpine; grant agreement number 825925, with Rebecca J. Williams, Frances C. Bach, Lisanne T. Laagland, Adel Medzikovic, Shaghayegh Basatvat, Nicolas Vedrenne, Joseph W. Snuggs, Deepani W. Poramba-Liyanage, Anne Camus, Marianna A. Tryfonidou, and Christine L. Le Maitre involved); it is also part of the project NC-CHOICE (with project number 19251 of the research program TTW which is partly financed by the Dutch Research Council (NWO). The financial support of the Dutch Arthritis Society (LLP22) is greatly appreciated. Danny Chan received funding from the RGC European Union – Hong Kong Research and Innovation Cooperation Co-Funding Mechanism (E-HKU703/18). Anne Camus received funding from Region Pays de la Loire, RFI BIOREGATE (CAVEODISC), and the French Society of Rheumatology (Spherodisc). The authors would like to thank the other members of the spine community whom contributed to early discussions of the article planning whom are authors from the prior NP methods paper.<sup>87</sup>

### CONFLICT OF INTEREST STATEMENT

The authors have no relevant conflicts of interest to declare in relation to this article.

### ORCID

Lisanne T. Laagland  <https://orcid.org/0000-0002-4456-6167>

Lily Paillat  <https://orcid.org/0009-0004-3598-9047>

Deepani W. Poramba-Liyanage  <https://orcid.org/0000-0003-3717-4787>

Anne Camus  <https://orcid.org/0000-0002-8820-0407>

Stephen M. Richardson  <https://orcid.org/0000-0002-7637-4135>

Marianna A. Tryfonidou  <https://orcid.org/0000-0002-2333-7162>

Christine L. Le Maitre  <https://orcid.org/0000-0003-4489-7107>

### REFERENCES

1. Balmer S, Nowotschin S, Hadjantonakis AK. Notochord morphogenesis in mice: current understanding and open questions. *Dev Dyn*. 2016;245(5):547-557. doi:10.1002/DVDY.24392

2. De Bree K, De Bakker BS, Oostra RJ. The development of the human notochord. *PLoS One*. 2018;13(10):e0205752. doi:[10.1371/JOURNAL.PONE.0205752](https://doi.org/10.1371/JOURNAL.PONE.0205752)
3. Camus A, Davidson BP, Billiards S, et al. The morphogenetic role of midline mesoderm and ectoderm in the development of the fore-brain and the midbrain of the mouse embryo. *Development*. 2000;127(9):1799-1813. doi:[10.1242/DEV.127.9.1799](https://doi.org/10.1242/DEV.127.9.1799)
4. Yamanaka Y, Tamplin OJ, Beckers A, Gossler A, Rossant J. Live imaging and genetic analysis of mouse notochord formation reveals regional morphogenetic mechanisms. *Dev Cell*. 2007;13(6):884-896. doi:[10.1016/J.DEVCEL.2007.10.016](https://doi.org/10.1016/J.DEVCEL.2007.10.016)
5. Lawson LY, Harfe BD. Developmental mechanisms of intervertebral disc and vertebral column formation. *Wiley Interdiscip Rev Dev Biol*. 2017;6(6):e283. doi:[10.1002/WDEV.283](https://doi.org/10.1002/WDEV.283)
6. Williams S, Alkhatib B, Serra R. Development of the axial skeleton and intervertebral disc. *Curr Top Dev Biol*. 2019;133:49-90. doi:[10.1016/BS.CTDB.2018.11.018](https://doi.org/10.1016/BS.CTDB.2018.11.018)
7. Copp AJ, Greene NDE, Murdoch JN. The genetic basis of mammalian neurulation. *Nat Rev Genet*. 2003;4(10):784-793. doi:[10.1038/nrg1181](https://doi.org/10.1038/nrg1181)
8. McCann MR, Séguin CA. Notochord cells in intervertebral disc development and degeneration. *J Dev Biol*. 2016;4(1):3. doi:[10.3390/jdb4010003](https://doi.org/10.3390/jdb4010003)
9. Tani S, Chung UI, Ohba S, Hojo H. Understanding paraxial mesoderm development and sclerotome specification for skeletal repair. *Exp Mol Med*. 2020;52(8):1166-1177. doi:[10.1038/s12276-020-0482-1](https://doi.org/10.1038/s12276-020-0482-1)
10. Ward L, Pang ASW, Evans SE, Stern CD. The role of the notochord in amniote vertebral column segmentation. *Dev Biol*. 2018;439(1):3-18. doi:[10.1016/j.ydbio.2018.04.005](https://doi.org/10.1016/j.ydbio.2018.04.005)
11. Wopat S, Bagwell J, Sumigray KD, et al. Spine patterning is guided by segmentation of the notochord sheath. *Cell Rep*. 2018;22(8):2026-2038. doi:[10.1016/j.celrep.2018.01.084](https://doi.org/10.1016/j.celrep.2018.01.084)
12. Choi KS, Cohn MJ, Harfe BD. Identification of nucleus pulposus precursor cells and notochordal remnants in the mouse: implications for disk degeneration and chordoma formation. *Dev Dyn*. 2008;237(12):3953-3958. doi:[10.1002/DVDY.21805](https://doi.org/10.1002/DVDY.21805)
13. McCann MR, Tamplin OJ, Rossant J, Séguin CA. Tracing notochord-derived cells using a Noto-cre mouse: implications for intervertebral disc development. *Dis Model Mech*. 2012;5(1):73-82. doi:[10.1242/DMM.008128](https://doi.org/10.1242/DMM.008128)
14. Lawson L, Harfe BD. Notochord to nucleus pulposus transition. *Curr Osteoporos Rep*. 2015;13(5):336-341. doi:[10.1007/S11914-015-0284-X](https://doi.org/10.1007/S11914-015-0284-X)
15. Bach FC, Poramba-Liyanaage DW, Riemers FM, et al. Notochordal cell-based treatment strategies and their potential in intervertebral disc regeneration. *Front Cell Dev Biol*. 2022;9:78049. doi:[10.3389/FCELL.2021.780749](https://doi.org/10.3389/FCELL.2021.780749)
16. Choi KS, Harfe BD. Hedgehog signaling is required for formation of the notochord sheath and patterning of nuclei pulposi within the intervertebral discs. *Proc Natl Acad Sci U S A*. 2011;108(23):9484-9489. doi:[10.1073/pnas.1007566108](https://doi.org/10.1073/pnas.1007566108)
17. Smits P, Lefebvre V. Sox5 and Sox6 are required for notochord extracellular matrix sheath formation, notochord cell survival and development of the nucleus pulposus of intervertebral discs. *Development*. 2003;130(6):1135-1148. doi:[10.1242/DEV.00331](https://doi.org/10.1242/DEV.00331)
18. Paavola LG, Wilson DB, Center EM. Histochemistry of the developing notochord, perichordal sheath and vertebrae in Danforth's short-tail (Sd) and normal C57BL/6 mice. *Development*. 1980;55(1):227-245. doi:[10.1242/DEV.55.1.227](https://doi.org/10.1242/DEV.55.1.227)
19. Richardson SM, Ludwinski FE, Gnanalingham KK, Atkinson RA, Freemont AJ, Hoyland JA. Notochordal and nucleus pulposus marker expression is maintained by sub-populations of adult human nucleus pulposus cells through aging and degeneration. *Sci Rep*. 2017;7(1):1501. doi:[10.1038/S41598-017-01567-W](https://doi.org/10.1038/S41598-017-01567-W)
20. Gan Y, He J, Zhu J, et al. Spatially defined single-cell transcriptional profiling characterizes diverse chondrocyte subtypes and nucleus pulposus progenitors in human intervertebral discs. *Bone Res*. 2021;9(1):1-15. doi:[10.1038/s41413-021-00163-z](https://doi.org/10.1038/s41413-021-00163-z)
21. Constant C, Hom WW, Nehrbass D, et al. Comparison and optimization of sheep in vivo intervertebral disc injury model. *JOR Spine*. 2022;5(2):e1198. doi:[10.1002/JSP2.1198](https://doi.org/10.1002/JSP2.1198)
22. Aguiar DJ, Johnson SL, Oegema TR. Notochordal cells interact with nucleus pulposus cells: regulation of proteoglycan synthesis. *Exp Cell Res*. 1999;246(1):129-137. doi:[10.1006/excr.1998.4287](https://doi.org/10.1006/excr.1998.4287)
23. Panebianco CJ, Dave A, Charytonowicz D, Sebra R, Iatridis JC. Single-cell RNA-sequencing atlas of bovine caudal intervertebral discs: discovery of heterogeneous cell populations with distinct roles in homeostasis. *FASEB J*. 2021;35(11):e21919. doi:[10.1096/FJ.202101149R](https://doi.org/10.1096/FJ.202101149R)
24. Hansen HJ. A pathologic-anatomical interpretation of disc degeneration in dogs. *Acta Orthop Scand*. 1951;20(4):280-293. doi:[10.3109/17453675108991175](https://doi.org/10.3109/17453675108991175)
25. Guehring T, Nerlich A, Kroeber M, Richter W, Omlor GW. Sensitivity of notochordal disc cells to mechanical loading: an experimental animal study. *Eur Spine J*. 2010;19(1):113-121. doi:[10.1007/S00586-009-1217-0](https://doi.org/10.1007/S00586-009-1217-0)
26. Scott NA, Harris PF, Bagnall KM. A morphological and histological study of the postnatal development of intervertebral discs in the lumbar spine of the rabbit. *J Anat*. 1980;130(Pt 1):75-81.
27. Adler JH, Schoenbaum M, Silberberg R. Early onset of disk degeneration and spondylosis in sand rats (*Psammomys obesus*). *Vet Pathol*. 1983;20(1):13-22. doi:[10.1177/030098588302000102](https://doi.org/10.1177/030098588302000102)
28. Winkler T, Mahoney EJ, Sinner D, Wylie CC, Dahia CL. Wnt signaling activates Shh signaling in early postnatal intervertebral discs, and re-activates Shh signaling in old discs in the mouse. *PLoS One*. 2014;9(6):e98444. doi:[10.1371/JOURNAL.PONE.0098444](https://doi.org/10.1371/JOURNAL.PONE.0098444)
29. Hunter CJ, Matyas JR, Duncan NA. Cytomorphology of notochordal and chondrocytic cells from the nucleus pulposus: a species comparison. *J Anat*. 2004;205(5):357-362. doi:[10.1111/j.0021-8782.2004.00352.x](https://doi.org/10.1111/j.0021-8782.2004.00352.x)
30. Trout JJ, Buckwalter JA, Moore KC, Landas SK. Ultrastructure of the human intervertebral disc. I. Changes in notochordal cells with age. *Tissue Cell*. 1982;14(2):359-369. doi:[10.1016/0040-8166\(82\)90033-7](https://doi.org/10.1016/0040-8166(82)90033-7)
31. Pattappa G, Li Z, Peroglio M, Wismer N, Alini M, Grad S. Diversity of intervertebral disc cells: phenotype and function. *J Anat*. 2012;221(6):480-496. doi:[10.1111/j.1469-7580.2012.01521.x](https://doi.org/10.1111/j.1469-7580.2012.01521.x)
32. Nerlich AG, Schleicher ED, Boos N. 1997 Volvo Award winner in basic science studies. Immunohistologic markers for age-related changes of human lumbar intervertebral discs. *Spine*. 1997;22(24):2781-2795. doi:[10.1097/00007632-199712150-00001](https://doi.org/10.1097/00007632-199712150-00001)
33. Bach F, de Vries S, Krouwels A, et al. The species-specific regenerative effects of notochordal cell-conditioned medium on chondrocyte-like cells derived from degenerated human intervertebral discs. *Eur Cells Mater*. 2015;30:132-147. doi:[10.22203/ECM.V030A10](https://doi.org/10.22203/ECM.V030A10)
34. Weiler C, Nerlich AG, Schaaf R, Bachmeier BE, Wuertz K, Boos N. Immunohistochemical identification of notochordal markers in cells in the aging human lumbar intervertebral disc. *Eur Spine J*. 2010;19(10):1761-1770. doi:[10.1007/S00586-010-1392-Z](https://doi.org/10.1007/S00586-010-1392-Z)
35. Bergmann W, de Lest C, van Plomp S, et al. Intervertebral disc degeneration in warmblood horses: histological and biochemical characterization. *Vet Pathol*. 2022;59(2):284-298. doi:[10.1177/03009858211067463](https://doi.org/10.1177/03009858211067463)
36. Hoogendoorn RJ, Wuisman PI, Smit TH, Everts VE, Helder MN. Experimental intervertebral disc degeneration induced by

- chondroitinase ABC in the goat. *Spine*. 2007;32(17):1816-1825. doi:[10.1097/BRS.0B013E31811EBAC5](https://doi.org/10.1097/BRS.0B013E31811EBAC5)
37. Shu C, Hughes C, Smith SM, et al. The ovine newborn and human foetal intervertebral disc contain perlecan and aggrecan variably substituted with native 7D4 CS sulphation motif: spatiotemporal immunolocalisation and co-distribution with Notch-1 in the human foetal disc. *Glycoconj J*. 2013;30(7):717-725. doi:[10.1007/S10719-013-9475-9](https://doi.org/10.1007/S10719-013-9475-9)
  38. Tam V, Chen P, Yee A, et al. DIPPER: a spatiotemporal proteomics atlas of human intervertebral discs for exploring ageing and degeneration dynamics. *Elife*. 2020;9:e64940. doi:[10.1101/2020.07.11.192948](https://doi.org/10.1101/2020.07.11.192948)
  39. Gilchrist CL, Darling EM, Chen J, Setton LA. Extracellular matrix ligand and stiffness modulate immature nucleus pulposus cell-cell interactions. *PLoS One*. 2011;6(11):e27170. doi:[10.1371/JOURNAL.PONE.0027170](https://doi.org/10.1371/JOURNAL.PONE.0027170)
  40. Risbud MV, Schoepflin ZR, Mwale F, et al. Defining the phenotype of young healthy nucleus pulposus cells: recommendations of the spine research interest group at the 2014 annual ORS meeting. *J Orthop Res*. 2015;33(3):283-293. doi:[10.1002/JOR.22789](https://doi.org/10.1002/JOR.22789)
  41. Hwang PY, Chen J, Jing L, Hoffman BD, Setton LA. The role of extracellular matrix elasticity and composition in regulating the nucleus pulposus cell phenotype in the intervertebral disc: a narrative review. *J Biomech Eng*. 2014;136(2):021010. doi:[10.1115/1.4026360](https://doi.org/10.1115/1.4026360)
  42. Peck SH, McKee KK, Tobias JW, Malhotra NR, Harfe BD, Smith LJ. Whole transcriptome analysis of notochord-derived cells during embryonic formation of the nucleus pulposus. *Scientific Reports*. 2017;7(1):1-14. doi:[10.1038/s41598-017-10692-5](https://doi.org/10.1038/s41598-017-10692-5)
  43. Wymeersch FJ, Skylaki S, Huang Y, et al. Transcriptionally dynamic progenitor populations organised around a stable niche drive axial patterning. *Development*. 2019;146(1):dev168161. doi:[10.1242/DEV.168161](https://doi.org/10.1242/DEV.168161)
  44. Rodrigues-Pinto R, Berry A, Piper-Hanley K, Hanley N, Richardson SM, Hoyland JA. Spatiotemporal analysis of putative notochordal cell markers reveals CD24 and keratins 8, 18, and 19 as notochord-specific markers during early human intervertebral disc development. *J Orthop Res*. 2016;34(8):1327-1340. doi:[10.1002/JOR.23205](https://doi.org/10.1002/JOR.23205)
  45. Rodrigues-Pinto R, Ward L, Humphreys M, et al. Human notochordal cell transcriptome unveils potential regulators of cell function in the developing intervertebral disc. *Sci Rep*. 2018;8(1):1-13. doi:[10.1038/s41598-018-31172-4](https://doi.org/10.1038/s41598-018-31172-4)
  46. Tessier S, Risbud MV. Understanding embryonic development for cell-based therapies of intervertebral disc degeneration: toward an effort to treat disc degeneration subphenotypes. *Dev Dyn*. 2021;250(3):302-317. doi:[10.1002/DVDY.217](https://doi.org/10.1002/DVDY.217)
  47. Jiang W, Glaeser JD, Salehi K, et al. Single-cell atlas unveils cellular heterogeneity and novel markers in human neonatal and adult intervertebral discs. *iScience*. 2022;25(7):104504. doi:[10.1016/J.ISCI.2022.104504](https://doi.org/10.1016/J.ISCI.2022.104504)
  48. Colombier P, Halgand B, Chédeville C, et al. NOTO transcription factor directs human induced pluripotent stem cell-derived Mesoderm progenitors to a Notochordal fate. *Cell*. 2020;9(2):509. doi:[10.3390/cells9020509](https://doi.org/10.3390/cells9020509)
  49. Zhang Y, Zhang Z, Chen P, et al. Directed differentiation of notochord-like and nucleus pulposus-like cells using human pluripotent stem cells. *Cell Rep*. 2020;30(8):2791-2806.e5. doi:[10.1016/j.celrep.2020.01.100](https://doi.org/10.1016/j.celrep.2020.01.100)
  50. Alini M, Diwan AD, Erwin WM, Little CB, Melrose J. An update on animal models of intervertebral disc degeneration and low back pain: exploring the potential of artificial intelligence to improve research analysis and development of prospective therapeutics. *JOR Spine*. 2023;6(1):e1230. doi:[10.1002/JSP2.1230](https://doi.org/10.1002/JSP2.1230)
  51. Smolders LA, Bergknut N, Grinwis GCM, et al. Intervertebral disc degeneration in the dog. Part 2: chondrodystrophic and non-chondrodystrophic breeds. *Veterinary Journal*. 2013;195(3):292-299. doi:[10.1016/J.TVJL.2012.10.011](https://doi.org/10.1016/J.TVJL.2012.10.011)
  52. Smolders LA, Meij BP, Onis D, et al. Gene expression profiling of early intervertebral disc degeneration reveals a down-regulation of canonical Wnt signaling and caveolin-1 expression: implications for development of regenerative strategies. *Arthritis Res Ther*. 2013;15(1):R23. doi:[10.1186/ar4157](https://doi.org/10.1186/ar4157)
  53. Bergknut N, Smolders LA, Grinwis GCM, et al. Intervertebral disc degeneration in the dog. Part 1: anatomy and physiology of the intervertebral disc and characteristics of intervertebral disc degeneration. *Vet J*. 2013;195(3):282-291. doi:[10.1016/j.tvjl.2012.10.024](https://doi.org/10.1016/j.tvjl.2012.10.024)
  54. Gantenbein-Ritter B, Chan SCW. The evolutionary importance of cell ratio between notochordal and nucleus pulposus cells: an experimental 3-D co-culture study. *Eur Spine J*. 2012;21(Suppl 6):819-825. doi:[10.1007/S00586-011-2026-9](https://doi.org/10.1007/S00586-011-2026-9)
  55. Gantenbein B, Calandriello E, Wuertz-Kozak K, Benneker LM, Keel MJB, Chan SCW. Activation of intervertebral disc cells by co-culture with notochordal cells, conditioned medium and hypoxia. *BMC Musculoskelet Disord*. 2014;15(1):422. doi:[10.1186/1471-2474-15-422](https://doi.org/10.1186/1471-2474-15-422)
  56. Williams RJ, Tryfonidou MA, Snuggs JW, Le Maitre CL. Cell sources proposed for nucleus pulposus regeneration. *JOR Spine*. 2021;4(4):e1175. doi:[10.1002/JSP2.1175](https://doi.org/10.1002/JSP2.1175)
  57. Purmessur D, Guterl CC, Cho SK, et al. Dynamic pressurization induces transition of notochordal cells to a mature phenotype while retaining production of important patterning ligands from development. *Arthritis Res Ther*. 2013;15(5):R122. doi:[10.1186/ar4302](https://doi.org/10.1186/ar4302)
  58. Potier E, Ito K. Using notochordal cells of developmental origin to stimulate nucleus pulposus cells and bone marrow stromal cells for intervertebral disc regeneration. *Eur Spine J*. 2014;23(3):679-688. doi:[10.1007/s00586-013-3107-8](https://doi.org/10.1007/s00586-013-3107-8)
  59. Arkesteijn ITM, Potier E, Ito K. The regenerative potential of Notochordal cells in a nucleus pulposus explant. *Global Spine J*. 2017;7(1):14-20. doi:[10.1055/s-0036-1583174](https://doi.org/10.1055/s-0036-1583174)
  60. Miyazaki T, Kobayashi S, Takeno K, Meir A, Urban J, Baba H. A phenotypic comparison of proteoglycan production of intervertebral disc cells isolated from rats, rabbits, and bovine tails; which animal model is most suitable to study tissue engineering and biological repair of human disc disorders? *Tissue Eng Part A*. 2009;15(12):3835-3846. doi:[10.1089/ten.tea.2009.0250](https://doi.org/10.1089/ten.tea.2009.0250)
  61. Kwon W-K, Moon HJ, Kwon T-H, Park Y-K, Kim JH. Influence of rabbit notochordal cells on symptomatic intervertebral disc degeneration: anti-angiogenic capacity on human endothelial cell proliferation under hypoxia. *Osteoarthr Cartil*. 2017;25:1738-1746. doi:[10.1016/j.joca.2017.06.003](https://doi.org/10.1016/j.joca.2017.06.003)
  62. Li XC, Wang MS, Liu W, et al. Co-culturing nucleus pulposus mesenchymal stem cells with notochordal cell-rich nucleus pulposus explants attenuates tumor necrosis factor- $\alpha$ -induced senescence. *Stem Cell Res Ther*. 2018;9(1):171. doi:[10.1186/s13287-018-0919-9](https://doi.org/10.1186/s13287-018-0919-9)
  63. Cappello R, Bird JLE, Pfeiffer D, Bayliss MT, Dudhia J. Notochordal cell produce and assemble extracellular matrix in a distinct manner, which may be responsible for the maintenance of healthy nucleus pulposus. *Spine*. 2006;31(8):873-882. doi:[10.1097/01.brs.0000209302.00820.fd](https://doi.org/10.1097/01.brs.0000209302.00820.fd)
  64. Spillekom S, Smolders LA, Grinwis GC, et al. Increased osmolarity and cell clustering preserve canine notochordal cell phenotype in culture. *Tissue Eng Part C*. 2014;20(8):652-662. doi:[10.1089/ten.tec.2013.0479](https://doi.org/10.1089/ten.tec.2013.0479)
  65. Kim JH, Deasy BM, Seo HY, et al. Differentiation of intervertebral Notochordal cells through live automated cell imaging system In vitro. *Spine*. 2009;34(23):2486-2493. doi:[10.1097/BRS.0b013e3181b26ed1](https://doi.org/10.1097/BRS.0b013e3181b26ed1)
  66. Potier E, de Vries S, van Doeselaar M, Ito K. Potential application of notochordal cells for intervertebral disc regeneration: an in vitro assessment. *Eur Cells Mater*. 2014;28:68-81. doi:[10.22203/eCM.v028a06](https://doi.org/10.22203/eCM.v028a06)

67. Wang JY, Baer AE, Kraus VB, Setton LA. Intervertebral disc cells exhibit differences in gene expression in alginate and monolayer culture. *Spine*. 2001;26(16):1747-1752. doi:10.1097/00007632-200108150-00003
68. Lee NN, Salzer E, Bach FC, et al. A comprehensive tool box for large animal studies of intervertebral disc degeneration. *JOR Spine*. 2021; 4(2):e1162. doi:10.1002/JSP2.1162
69. Hubrecht RC, Carter E. The 3Rs and humane experimental technique: implementing change. *Animals (Basel)*. 2019;9(10):754. doi:10.3390/ANI9100754
70. Thorpe A, Bach F, Tryfonidou M, et al. Leaping the hurdles in developing regenerative treatments for the intervertebral disc from pre-clinical to clinical. *JOR Spine*. 2018;1(3):e1027. doi:10.1002/jsp2.1027
71. Snuggs JW, Day RE, Bach FC, et al. Aquaporin expression in the human and canine intervertebral disc during maturation and degeneration. *JOR Spine*. 2019;2(1):e1049. doi:10.1002/jsp2.1049
72. Hunter CJ, Matyas JR, Duncan NA. The notochordal cell in the nucleus pulposus: a review in the context of tissue engineering. *Tissue Eng*. 2003;9(4):667-677. doi:10.1089/107632703768247368
73. Hunter CJ, Matyas JR, Duncan NA. The three-dimensional architecture of the notochordal nucleus pulposus: novel observations on cell structures in the canine intervertebral disc. *J Anat*. 2003;202(3):279-291. doi:10.1046/j.1469-7580.2003.00162.x
74. Hunter CJ, Matyas JR, Duncan NA. The functional significance of cell clusters in the Notochordal nucleus pulposus: survival and signaling in the canine intervertebral disc. *Basic Sci*. 2004;29(10):1099-1104.
75. Hwang PY, Jing L, Michael KW, Richardson WJ, Chen J, Setton LA. N-cadherin-mediated signaling regulates cell phenotype for nucleus pulposus cells of the intervertebral disc. *Cell Mol Bioeng*. 2015;8(1): 51-62. doi:10.1007/s12195-014-0373-4
76. Kothari S, Chaudry Q, Wang MD. Automated cell counting and cluster segmentation using concavity detection and ellipse fitting techniques. *Proc IEEE Int Symp Biomed Imaging*. 2009;2009:795-798.
77. Ohnuma K, Fujiki A, Yanagihara K, et al. Enzyme-free passage of human pluripotent stem cells by controlling divalent cations. *Sci Rep*. 2014;4:4646. doi:10.1038/srep04646
78. Wallman L, Åkesson E, Ceric D, et al. Biogrid-a microfluidic device for large-scale enzyme-free dissociation of stem cell aggregates. *Lab Chip*. 2011;11(19):3241-3248. doi:10.1039/c1lc20316a
79. Beers J, Gulbranson DR, George N, et al. Passaging and colony expansion of human pluripotent stem cells by enzyme-free dissociation in chemically defined culture conditions. *Nat Protoc*. 2012;7(11): 2029-2040. doi:10.1038/nprot.2012.130
80. Ellerström C, Strehl R, Noaksson K, Hyllner J, Semb H. Facilitated expansion of human embryonic stem cells by single-cell enzymatic dissociation. *Stem Cells*. 2007;25(7):1690-1696. doi:10.1634/stemcells.2006-0607
81. Lin CH, Lee DC, Chang HC, Chiu IM, Hsu CH. Single-cell enzyme-free dissociation of neurospheres using a microfluidic chip. *Anal Chem*. 2013;85(24):11920-11928. doi:10.1021/ac402724b
82. Diaz-Hernandez ME, Khan NM, Trochez CM, et al. Derivation of notochordal cells from human embryonic stem cells reveals unique regulatory networks by single cell-transcriptomics. *J Cell Physiol*. 2020;235(6):5241-5255. doi:10.1002/jcp.29411
83. Jager LD, Canda CMA, Hall CA, et al. Effect of enzymatic and mechanical methods of dissociation on neural progenitor cells derived from induced pluripotent stem cells. *Adv Med Sci*. 2016; 61(1):78-84. doi:10.1016/j.advms.2015.09.005
84. Tamagawa S, Sakai D, Schol J, et al. N-acetylcysteine attenuates oxidative stress-mediated cell viability loss induced by dimethyl sulfide in cryopreservation of human nucleus pulposus cells: a potential solution for mass production. *JOR Spine*. 2022;5(4):e1223. doi: 10.1002/JSP2.1223
85. Croft AS, Guerrero J, Oswald KAC, Häckel S, Albers CE, Gantenbein B. Effect of different cryopreservation media on human nucleus pulposus cells' viability and trilineage potential. *JOR Spine*. 2021;4(1):e1140. doi:10.1002/JSP2.1140
86. Nukaga T, Sakai D, Tanaka M, Hiyama A, Nakai T, Mochida J. Transplantation of activated nucleus pulposus cells after cryopreservation: efficacy study in a canine disc degeneration model. *Eur Cells Mater*. 2016;31:95-106. doi:10.22203/eCM.v031a07
87. Basatvat S, Bach FC, Barcellona MN, et al. Harmonization and standardization of nucleus pulposus cell extraction and culture methods. *JOR Spine*. 2023;6:e1238. doi:10.1002/JSP2.1238
88. Hunter CJ, Bianchi S, Cheng P, Muldrew K. Osmoregulatory function of large vacuoles found in notochordal cells of the intervertebral disc running title: an osmoregulatory vacuole. *MCB Mol Cell Biomech*. 2007;4(4):227-237. doi:10.3970/mcb.2007.004.227
89. Inaba Y, Aikawa Y, Hirai T, et al. In-straw cryoprotectant dilution for bovine embryos vitrified using Cryotop. *J Reprod Dev*. 2011;57(4): 437-443. doi:10.1262/JRD.10-154M
90. Mahmoud KGM, Scholkamy TH, Ahmed YF, Seidel GE, Nawito MF. Effect of different combinations of Cryoprotectants on In vitro maturation of immature Buffalo (*Bubalus bubalis*) oocytes vitrified by straw and open-pulled straw methods. *Reprod Domest Anim*. 2010; 45(4):565-571. doi:10.1111/J.1439-0531.2008.01293.X
91. Dahia CL, Mahoney E, Wylie C. Shh signaling from the nucleus pulposus is required for the postnatal growth and differentiation of the mouse intervertebral disc. *PLoS One*. 2012;7(4):e35944. doi:10.1371/JOURNAL.PONE.0035944
92. Maier JA, Lo YT, Harfe BD. Foxa1 and Foxa2 are required for formation of the intervertebral discs. *PLoS One*. 2013;8(1):55528. doi:10.1371/JOURNAL.PONE.0055528
93. Risbud MV, Schaer TP, Shapiro IM. Toward an understanding of the role of notochordal cells in the adult intervertebral disc: from discord to accord. *Dev Dyn*. 2010;239(8):2141-2148. doi:10.1002/DVDY.22350
94. Hwang PY, Jing L, Chen J, et al. N-cadherin is key to expression of the nucleus pulposus cell phenotype under selective substrate culture conditions. *Sci Rep*. 2016;6:28038. doi:10.1038/SREP28038
95. Bach FC, Zhang Y, Miranda-Bedate A, et al. Increased caveolin-1 in intervertebral disc degeneration facilitates repair. *Arthritis Res Ther*. 2016;18(1):59. doi:10.1186/S13075-016-0960-Y
96. Heathfield SK, Le Maitre CL, Hoyland JA. Caveolin-1 expression and stress-induced premature senescence in human intervertebral disc degeneration. *Arthritis Res Ther*. 2008;10(4):R87. doi:10.1186/AR2468
97. Paillat L, Coutant K, Dutilleul M, Le Lay S, Camus A. Three-dimensional culture model to study the biology of vacuolated notochordal cells from mouse nucleus pulposus explants. *Eur Cell Mater*. 2023;45:72-87. doi:10.22203/ECM.V045A06
98. Bagwell J, Norman J, Ellis K, et al. Notochord vacuoles absorb compressive bone growth during zebrafish spine formation. *Elife*. 2020; 9:51221. doi:10.7554/eLife.51221
99. Thorpe A, Binch A, Creemers L, Sammon C, Le Maitre C. Nucleus pulposus phenotypic markers to determine stem cell differentiation: fact or fiction? *Oncotarget*. 2016;7(3):2189-2200. doi:10.18632/oncotarget.6782
100. Kalinichenko VV, Gusarova GA, Shin B, Costa RH. The forkhead box F1 transcription factor is expressed in brain and head mesenchyme during mouse embryonic development. *Gene Expr Patterns*. 2003; 3(2):153-158. doi:10.1016/S1567-133X(03)00010-3
101. Beckers A, Alten L, Viebahn C, Andre P, Gossler A. The mouse homeobox gene Noto regulates node morphogenesis, notochordal ciliogenesis, and left right patterning. *Proc Natl Acad Sci U S A*. 2007; 104(40):15765-15770. doi:10.1073/PNAS.0704344104
102. Götz W, Kasper M, Miosge N, Hughes RC. Detection and distribution of the carbohydrate binding protein galectin-3 in human notochord, intervertebral disc and chordoma. *Differentiation*. 1997;62(3): 149-157. doi:10.1046/J.1432-0436.1997.6230149.X

103. McMahon JA, Takada S, Zimmerman LB, Fan CM, Harland RM, McMahon AP. Noggin-mediated antagonism of BMP signaling is required for growth and patterning of the neural tube and somite. *Genes Dev.* 1998;12(10):1438-1452. doi:[10.1101/GAD.12.10.1438](https://doi.org/10.1101/GAD.12.10.1438)
104. Ben Abdelkhalek H, Beckers A, Schuster-Gossler K, et al. The mouse homeobox gene *not* is required for caudal notochord development and affected by the truncate mutation. *Genes Dev.* 2004;18(14):1725-1736. doi:[10.1101/GAD.303504](https://doi.org/10.1101/GAD.303504)
105. Bach FC, de Rooij KM, Riemers FM, et al. Hedgehog proteins and parathyroid hormone-related protein are involved in intervertebral disc maturation, degeneration, and calcification. *JOR Spine.* 2019;2(4):e1071. doi:[10.1002/JSP2.1071](https://doi.org/10.1002/JSP2.1071)
106. Takimoto A, Kokubu C, Watanabe H, et al. Differential transactivation of the upstream aggrecan enhancer regulated by PAX1/9 depends on SOX9-driven transactivation. *Sci Rep.* 2019;9(1):4605. doi:[10.1038/S41598-019-40810-4](https://doi.org/10.1038/S41598-019-40810-4)
107. Barrionuevo F, Taketo MM, Scherer G, Kispert A. Sox9 is required for notochord maintenance in mice. *Dev Biol.* 2006;295(1):128-140. doi:[10.1016/J.YDBIO.2006.03.014](https://doi.org/10.1016/J.YDBIO.2006.03.014)
108. Xu G, Liu Y, Zhang C, et al. Temporal and spatial expression of Sox9, Pax1, TGF- $\beta$ 1 and type I and II collagen in human intervertebral disc development. *Neurochirurgie.* 2020;66(3):168-173. doi:[10.1016/J.NEUCHI.2019.12.011](https://doi.org/10.1016/J.NEUCHI.2019.12.011)
109. Sive JI, Baird P, Jeziorski M, Watkins A, Hoyland JA, Freemont AJ. Expression of chondrocyte markers by cells of normal and degenerate intervertebral discs. *Mol Pathol.* 2002;55(2):91-97. doi:[10.1136/MP.55.2.91](https://doi.org/10.1136/MP.55.2.91)
110. Le Maitre CL, Hoyland JA, Freemont AJ. Studies of human intervertebral disc cell function in a constrained in vitro tissue culture system. *Spine.* 2004;29(11):1187-1195. doi:[10.1097/00007632-200406010-00006](https://doi.org/10.1097/00007632-200406010-00006)
111. Gruber HE, Norton HJ, Ingram JA, Hanley EN. The SOX9 transcription factor in the human disc: decreased immunolocalization with age and disc degeneration. *Spine.* 2005;30(6):625-630. doi:[10.1097/01.BRS.0000155420.01444.C6](https://doi.org/10.1097/01.BRS.0000155420.01444.C6)
112. Kudelko M, Chen P, Tam V, et al. PRIMUS: comprehensive proteomics of mouse intervertebral discs that inform novel biology and relevance to human disease modelling. *Matrix Biol plus.* 2021;12:12. doi:[10.1016/J.MBPLUS.2021.100082](https://doi.org/10.1016/J.MBPLUS.2021.100082)
113. Hayes AJ, Benjamin M, Ralphs JR. Extracellular matrix in development of the intervertebral disc. *Matrix Biol.* 2001;20(2):107-121. doi:[10.1016/S0945-053X\(01\)00125-1](https://doi.org/10.1016/S0945-053X(01)00125-1)
114. Roughley PJ, Geng Y, Mort JS. The non-aggregated aggrecan in the human intervertebral disc can arise by a non-proteolytic mechanism. *Eur Cell Mater.* 2014;28:129-136. doi:[10.22203/ECM.V028A10](https://doi.org/10.22203/ECM.V028A10)
115. Palacio-Mancheno PE, Evashwick-Rogler TW, Laudier DM, Purmessur D, Iatridis JC. Hyperosmolarity induces notochordal cell differentiation with aquaporin3 upregulation and reduced N-cadherin expression. *J Orthop Res.* 2018;36(2):788-798. doi:[10.1002/JOR.23715](https://doi.org/10.1002/JOR.23715)
116. Bach FC, Tellegen AR, Beukers M, et al. Biologic canine and human intervertebral disc repair by notochordal cell-derived matrix: from bench towards bedside. *Oncotarget.* 2018;9(41):26507-26526. doi:[10.18632/oncotarget.25476](https://doi.org/10.18632/oncotarget.25476)
117. Perris R, Kuo H-J, Glanville RW, Bronner-Fraser M. Collagen type VI in neural crest development: distribution in situ and interaction with cells in vitro. *Dev Dyn.* 1993;198(2):135-149. doi:[10.1002/AJA.1001980207](https://doi.org/10.1002/AJA.1001980207)
118. Aulisa L, Tamburrelli F, Lupporelli S, Tartarone M, Padua R. Immunohistochemical investigation on type III and VI collagen organization in human intervertebral discs in the neonatal period. *Child Nerv Syst.* 1998;14(3):104-108. doi:[10.1007/S003810050188](https://doi.org/10.1007/S003810050188)
119. Nerlich AG, Boos N, Wiest I, Aebi M. Immunolocalization of major interstitial collagen types in human lumbar intervertebral discs of various ages. *Virchows Archiv.* 1998;432(1):67-76. doi:[10.1007/S004280050136](https://doi.org/10.1007/S004280050136)
120. Tsingas M, Ottone OK, Haseeb A, et al. Sox9 deletion causes severe intervertebral disc degeneration characterized by apoptosis, matrix remodeling, and compartment-specific transcriptomic changes. *Matrix Biol.* 2020;94:110-133. doi:[10.1016/J.MATBIO.2020.09.003](https://doi.org/10.1016/J.MATBIO.2020.09.003)
121. Rajpurohit R, Risbud MV, Ducheyne P, Vresilovic EJ, Shapiro IM. Phenotypic characteristics of the nucleus pulposus: expression of hypoxia inducing factor-1, glucose transporter-1 and MMP-2. *Cell Tissue Res.* 2002;308(3):401-407. doi:[10.1007/s00441-002-0563-6](https://doi.org/10.1007/s00441-002-0563-6)
122. Richardson SM, Knowles R, Tyler J, Mobasher A, Hoyland JA. Expression of glucose transporters GLUT-1, GLUT-3, GLUT-9 and HIF-1 $\alpha$  in normal and degenerate human intervertebral disc. *Histochem Cell Biol.* 2008;129(4):503-511. doi:[10.1007/S00418-007-0372-9](https://doi.org/10.1007/S00418-007-0372-9)
123. Sakai D, Nakamura Y, Nakai T, et al. Exhaustion of nucleus pulposus progenitor cells with ageing and degeneration of the intervertebral disc. *Nat Commun.* 2012;3:1264. doi:[10.1038/NCOMMS2226](https://doi.org/10.1038/NCOMMS2226)
124. Sakai D, Schol J, Bach FC, et al. Successful fishing for nucleus pulposus progenitor cells of the intervertebral disc across species. *JOR Spine.* 2018;1(2):e1018. doi:[10.1002/jsp2.1018](https://doi.org/10.1002/jsp2.1018)
125. Tekari A, Chan SCW, Sakai D, Grad S, Gantenbein B. Angiopoietin-1 receptor Tie2 distinguishes multipotent differentiation capability in bovine coccygeal nucleus pulposus cells. *Stem Cell Res Ther.* 2016;7(1):75. doi:[10.1186/s13287-016-0337-9](https://doi.org/10.1186/s13287-016-0337-9)
126. Lama P, Claireaux H, Flower L, et al. Physical disruption of intervertebral disc promotes cell clustering and a degenerative phenotype. *Cell Death Discov.* 2019;5(1):1-9. doi:[10.1038/s41420-019-0233-z](https://doi.org/10.1038/s41420-019-0233-z)
127. Le MCL, Dahia CL, Giers M, et al. Development of a standardized histopathology scoring system for human intervertebral disc degeneration: an Orthopaedic Research Society spine section initiative. *JOR Spine.* 2021;4(2):e1167. doi:[10.1002/JSP2.1167](https://doi.org/10.1002/JSP2.1167)
128. Brown S, Matta A, Erwin M, et al. Cell clusters are indicative of stem cell activity in the degenerate intervertebral disc: can their properties be manipulated to improve intrinsic repair of the disc? *Stem Cells Dev.* 2018;27(3):147-165. doi:[10.1089/SCD.2017.0213](https://doi.org/10.1089/SCD.2017.0213)
129. Johnson WEB, Eisenstein SM, Roberts S. Cell cluster formation in degenerate lumbar intervertebral discs is associated with increased disc. *Cell Prolif.* 2009;42(3):197-207. doi:[10.3109/03008200109005650](https://doi.org/10.3109/03008200109005650)
130. Garcia J, Bagwell J, Njaine B, et al. Sheath cell invasion and transdifferentiation repair mechanical damage caused by loss of Caveolae in the zebrafish notochord. *Curr Biol.* 2017;27(13):1982-1989.e3. doi:[10.1016/j.cub.2017.05.035](https://doi.org/10.1016/j.cub.2017.05.035)
131. Pollard SM, Parsons MJ, Kamei M, et al. Essential and overlapping roles for laminin  $\alpha$  chains in notochord and blood vessel formation. *Dev Biol.* 2006;289(1):64-76. doi:[10.1016/j.ydbio.2005.10.006](https://doi.org/10.1016/j.ydbio.2005.10.006)
132. Corallo D, Schiavinato A, Trapani V, Moro E, Argenton F, Bonaldo P. Emilin3 is required for notochord sheath integrity and interacts with Scube2 to regulate notochord-derived hedgehog signals. *Development.* 2013;140(22):4594-4601. doi:[10.1242/dev.094078](https://doi.org/10.1242/dev.094078)
133. Gansner JM, Gitlin AJD. Essential role for the alpha 1 chain of type VIII collagen in zebrafish notochord formation. *Dev Dyn.* 2008;237(12):3715-3726. doi:[10.1002/dvdy.21779](https://doi.org/10.1002/dvdy.21779)
134. Parsons MJ, Pollard SM, Saude L, et al. Zebrafish mutants identify an essential role for laminins in notochord formation. *Development.* 2002;129(13):3137-3146.
135. Maître JL, Heisenberg CP. Three functions of cadherins in cell adhesion. *Curr Biol.* 2013;23(14):R626-R633. doi:[10.1016/j.cub.2013.06.019](https://doi.org/10.1016/j.cub.2013.06.019)

136. Binch A, Snuggs J, Le Maitre CL. Immunohistochemical analysis of protein expression in formalin fixed paraffin embedded human intervertebral disc tissues. *JOR Spine*. 2020;3(3):e1098. doi:[10.1002/JSP2.1098](https://doi.org/10.1002/JSP2.1098)
137. Humphreys MD, Ward L, Richardson SM, Hoyland JA. An optimized culture system for notochordal cell expansion with retention of phenotype. *JOR Spine*. 2018;1(3):e1028. doi:[10.1002/jsp2.1028](https://doi.org/10.1002/jsp2.1028)

#### SUPPORTING INFORMATION

Additional supporting information can be found online in the Supporting Information section at the end of this article.

**How to cite this article:** Williams, R. J., Laagland, L. T., Bach, F. C., Ward, L., Chan, W., Tam, V., Medzikovic, A., Basatvat, S., Paillat, L., Vedrenne, N., Snuggs, J. W., Poramba-Liyanage, D. W., Hoyland, J. A., Chan, D., Camus, A., Richardson, S. M., Tryfonidou, M. A., & Le Maitre, C. L. (2023).

Recommendations for intervertebral disc notochordal cell investigation: From isolation to characterization. *JOR Spine*, 6(3), e1272. <https://doi.org/10.1002/jsp2.1272>